Tracing foot-and-mouth disease virus phylogeographical patterns and transmission dynamics.

Manuel Jara
North Carolina State University
Alba Frias-De-Diego
North Carolina State University
Simon Dellicour
"Universite Libre de Bruxelles"
Guy Baele
Rega Institute
Gustavo Machado (gmachad@ncsu.edu)
University of Minnesota College of Veterinary Medicine https://orcid.org/0000-0001-7552-6144

Research article

Keywords: molecular epidemiology, transboundary emerging diseases, virus dispersal

Posted Date: January 9th, 2020

DOI: https://doi.org/10.21203/rs.2.20387/v1

Abstract

Background

Foot-and-mouth disease virus (FMDV) has proven its potential to propagate across local and international borders on numerous occasions, but yet details about the directionality of the spread along with the role of the different host in transmission remain unexplored. To elucidate FMDV global spread characteristics, we studied the spatiotemporal phylodynamics of serotypes O, A, Asia1, SAT1, SAT2, and SAT3, based on more than 50 years of phylogenetic and epidemiological information.

Results

Our results revealed phylogeographic patterns, dispersal rates, and the role of host species in the dispersal and maintenance of virus circulation. Contrary to previous studies, our results showed that three serotypes were monophyletic (O, A, and Asia1), while all SATs serotypes did not evidence a defined common ancestor. Root state posterior probability (RSPP) analysis suggested Belgium as the country of origin for serotype O (RSPP= 0.27). India was the ancestral country for serotypes A (RSPP= 0.28), and Asia-1 (RSPP= 0.34), while Uganda appeared as the most likely origin country of all SAT serotypes (RSPP> 0.45). Furthermore, we identified the key centers of dispersal of the virus, being China, India and Uganda the most important ones. Bayes factor analysis revealed cattle as the major source of the virus for most of the serotypes (RSPP> 0.63), where the most important host-species transition route for serotypes O, A, and Asia1 was from cattle Bos taurus to swine Sus scrofa domesticus (BF>500), while, for SAT serotypes was from B. taurus to African buffalo Syncerus caffer.

Conclusions

This study provides significant insights into the spatiotemporal dynamics of the global circulation of FMDV serotypes, by characterizing the viral routes of spread at serotype level, especially uncovering the importance of host species for each serotype in the evolution and spread of FMDV which further improve future decisions for more efficient control and eradication.

Introduction

The rapid growth of global population along with the current demand for animal protein and the increasing animal trade have increased the spread of a broad range of transboundary animal diseases (TADs) [1, 2]. Clear examples of this phenomenon are the recent emergence of African Swine Fever in Asia, Avian Influenza or Contagious Bovine Pleuropneumonia and the return of Foot-and-mouth disease virus (FMDV) to Korea and other countries which successfully eliminated the virus for several years [3–7]. Understanding the tempo and mode of disease evolution allows to estimate the impact of external factors influencing these diseases and assess the evolutionary patterns followed over time, which can be better studied by considering the most recent advances in virus sequencing and phylogenetics [8–10].

Molecular phylogenetics has shown to be an accurate and highly impacting approach in the understanding of the spatiotemporal dynamics of infectious diseases, with the capacity to explain disease spread, virulence and invasion potential [11–20]. In the case of TADs, molecular phylogenetics has also proven to be a useful approach, providing accurate knowledge for the control of pathogens worldwide [21–24], however, it remains underused.

FMDV causes the most influential transboundary animal disease with historical worldwide circulation reported in domestic and wildlife reservoirs [25, 26]. FMD is a highly contagious disease caused by a small single-stranded RNA virus of the genus *Aphthovirus*, member of the family Picornaviridae [27] and classified into seven different serotypes; O, A, C, Asia1 and Southern African Territories (SATs) 1, 2 and 3 [25, 28–30] which severely affect the productivity of domesticated livestock, causing great economic losses [31–33]. The United States Department of Agriculture has estimated that the introduction of FMDV could result in losses between $15 to $100 billion [34–37]. One of the main reasons for this great impact is the wide variety of hosts known for FMDV (i.e., cattle, buffalo, swine, sheep, and deer), altogether it affects more than 70 species of cloven-hoofed animals [38]. FMDV is known to be transmitted locally and globally, often associated with infected animal products and human and animal movements [39, 40]. Transmission is also facilitated by airborne spread, direct animal contact with infected individuals or carcasses and translocation of contaminated staff, equipment, and machinery [41, 42].

Individual genes have been widely used to study the phylogenetic relationships among FMD serotypes [43–50], however, little has been done using whole genome sequences (WGS) [26, 51–53]. Nevertheless, these studies have been often based on a limited number of sequences (<200), or on phylogenetic methods that do not have the ability to accommodate uncertainty (i.e., Bayesian phylodynamic methods) [54]. Although these methods have been widely used, they present certain degree of evolutionary inaccuracy since in most cases (excluding [50] and [48]) the Bayesian phylogenetic and phylodynamic methods were not considered. Thus, their inherent ability to accommodate uncertainty, and therefore to assess the level of error of the predictions obtained, was often neglected.

Several studies have explored the spatiotemporal evolutionary dynamics of FMDV in different parts of the world, mainly focusing on the diffusion patterns across its endemic regions: Asia and Africa [31, 48, 55–59] However, studies considering all serotypes are only available within small geographic regions, and global studies only assessed some of the viral serotypes [55, 60].

In this study, we investigated the spatiotemporal dynamics of FMDV by using Bayesian phylodynamic analyses of comprehensive genetic, geographical and temporal data regarding past FMDV occurrences. The objectives of this work were to reconstruct the global evolutionary epidemiology of FMDV serotypes O, A, Asia1, and SATs, to make comparisons among the global spatiotemporal spread of each FMDV serotype, identify ancestral countries and provide inferences about the evolutionary patterns and the transmission between host species.

Methods

Data collection and curation

Genetic and geographical information of FMDV was obtained from the Virus Pathogen Resource database, available at https://www.viprbrc.org (See Table S1). Despite the original dataset consisted on 688 whole genome sequences (WGS), we manually removed all duplicated sequences (to have just one sample per FMDV outbreak) (See Table S2). Thus, we built a comprehensive dataset comprising 249 WGS that gather information from 43 countries and 4 continents. This dataset includes information of six FMDV serotypes (A, O, Asia1, SAT 1, SAT 2 and SAT 3), with collection dates ranging from 1905 to 2019 (GenBank ID numbers in Supplementary material Table S1). Serotype C was not included in this study due to low data unavailability (only 3 sequences were available). To determine accurate phylogenetic relationships among FMDV reports, we combined the available genetic information along with collection date, host species (i.e., *Bos taurus*= cattle, *Syncerus caffer*= African buffalo, *Bubalus bubalis*= Water buffalo, *Sus scrofa domesticus*= swine, *Sus scrofa*= boar, and *Ovis aries*= sheep) and location (discrete information at country level) as metadata information. Any sample lacking one of these three characteristics was discarded.

Discrete phylogeographical analysis

Sequences were aligned using Mega X, available at www.megasoftware.net [61]. The recombination detection program (RDP) v5.3 was used to search for evidence of recombination within our dataset [62]. Each serotype was screened using five different methods (BootScan, Chimaera, MaxChi, RDP, and SiScan). To reduce the bias generated by the strong unbalance of the available data in both dimensions (i.e., number of samples per country and uneven number of samples per host species), we removed all the sequences that where duplicated (i.e., represented the same outbreak multiple times), which, in the case of big outbreaks such as United Kingdom 2001/2007, Argentina 2001, and Japan 2010, accounted for hundreds of sequences representing each event. We found no evidence of recombinant sequences in any FMDV serotypes analyzed. To determine whether there was a sufficient temporal molecular evolutionary signal of the FMDV sequences used for each serotype phylogeny, we used TempEst v1.5 [63]. To calculate the *P*-values associated with the phylogenetic signal analysis, we used the approach described by [64] based on 1,000 random permutations of the sequence sampling dates [65]. The relationship found between root-to-tip divergence and sampling dates (years) supported the use of molecular clock analysis in this study for all serotypes. Root-to-tip regression results for each serotype are reported in Supplementary Table S3, all the results supported a significant temporal signal (P-value<0.05). Phylogeographic history of FMDV dispersal was recovered from the obtained spatiotemporal phylogenies for each serotype. Phylogenetic trees were generated by a discrete phylogeography estimation by Bayesian inference through Markov chain Monte Carlo (MCMC), implemented in BEAST v2.5.0 [66]. We partitioned the coding genes into first + second and third codon positions and applied a separate Hasegawa-Kishino-Yano (HKY+G; [67]) substitution model with gamma-distributed rate heterogeneity among sites to each partition [68].

By using Nested Sampling Beast package v1.0.4 [69] we compared different molecular clock models to find the one that showed the best fit for the data related to each serotype. The marginal likelihood value supported the use of uncorrelated lognormal relaxed molecular clock [70]. To infer the epidemic demographic histories of FMDV per each serotype we estimated the effective number of infections through time by using the Bayesian skyline plot approach [71]. All analyses were developed for 200 million generations, sampling every 10,000th generation and removing 10% as chain burn-in. All the Markov chain Monte Carlo analyses for each serotype were investigated using Tracer software v1.7 [72] to ensure adequate effective sample sizes (ESS) (above 200), which were obtained for all parameters. Final trees were summarized and visualized via Tree Annotator v. 2.3.0 and FigTree 1.4.3 respectively (included in BEAST v2.5.0) [66, 73].

To reconstruct the ancestral-state phylogeographic transmission across countries and hosts, we used the discrete-trait extension implemented in BEASTv2.5.0 [66]. In addition, to explore the most important historical dispersal routes for the spread FMDV across countries, as well as most probable host-species transition, we used a Bayesian stochastic search variable selection (BSSVS) [74]. Using BSSVS approach, we identified and eliminated the nonzero rates of change between each pair of discrete traits (countries and hosts species) based on its Bayes factor value obtained (lower than 3). To perform this analysis, a symmetric rate matrix was assumed. To infer the intensity of directional transitions (forward and backward) within a matrix of the discrete traits mentioned above, we used a Markov jumps approach. To interpret the Bayes factors, a value of <3, as mentioned above, is not significant (hardly worth mentioning), BF= 3.1-20 represents positive support, BF= 20.1-150 represents strong support, while >150.1 represents an overwhelming support [75].

Finally, we visualized the spatiotemporal viral diffusion of each serotype by using Spatial Phylogenetic Reconstruction of Evolutionary Dynamics using Data-Driven Documents (D3) SPREAD3 software [76] considering the whole transmission and also the most significant connections between localities following the BSSVS method, with each country used as a discrete variable with a cutoff BF > 3 [75]. In addition, we classified the viral spread of each serotype in two categories: local, if the transmission occurs through neighboring countries, and long distance, if the dispersion jumps beyond adjacent neighboring countries.

Availability of data and materials

All the sequences including country of origin, host and date are comes from Virus Pathogen Resource database, available at https://www.viprbrc.org. In addition, all the data used in this study is part of the supplementary material (See Table S1).

Results

The number of available sequences per country varied from 1 to 18 WGS. Our results showed that India, China, Uganda, Argentina, and Zimbabwe were the countries with the highest number of available genomes (Supplementary Table S2). Likewise, several countries have been historically affected by more than one serotype, particularly in Africa and Asia, where we observed that Uganda presented the highest virus diversity as it has been subjected to the spread of serotypes O, and all SATs (Supplementary Table S2, Supplementary Fig. S1).

Spatiotemporal dynamics of FMDV

Phylogeographic analyses highlighted great asymmetries in the tempo and mode of each serotype evolution (Fig. 1). SAT1 appeared to be the basal clade of the entire lineage, originating SAT2, SAT3 and serotype A, which later diversified into serotype Asia1, and O. Our analysis suggested O as the most recent, prolific and widespread lineage, with the highest number of sequences available worldwide. Serotype A and Asia1 appeared second and third in the number of available sequences, followed by all SAT serotypes. Maximum clade credibility phylogeny showed the monophyly of serotypes O, A, and Asia1 (each serotype shared a common ancestor), while SAT serotypes appeared to have multiple origins (Fig. 1).

Spatiotemporal diffusion among serotypes

We investigated and compared the historical spreads of FMDV at serotype level, from the ones with local distribution (Asia1 and SATs) to the serotypes with widespread dispersal (O and A) [26, 28, 34, 55, 77, 78].

Serotype O

We analyzed 97 WGS from serotype O, which comprises 39% of the global FMDV tree (Fig. 1). This serotype also presents the widest distribution of all serotypes, with records from 42 countries (Fig. 2). Based on our phylogeographic analysis, the most likely center of origin for this serotype was Belgium (RSPP= 0.27) from which it spread globally across long distances to several countries through Europe, Asia, Africa and South America. A remarkable aspect of this global spread is that most of it has occurred in less than 50 years (Fig. 3A) (see Supplementary Video S1 for detailed footage). These patterns have also appeared in our spatiotemporal diffusion map, which shows that the global distribution of this serotype is highly represented by long-range movements across countries and continents (Fig. 3A). Phylogenetic reconstruction identified clusters formed by different sub-lineages, where the most representative centers of dispersal events (geographic spread accompanied by diversification) for this serotype were Poland and the United Kingdom in Europe, China, Japan, and Indonesia in Asia, Egypt in Africa and Argentina in South America. Likewise, we observed that China, South Korea, and Turkey were also among the countries with the highest number of sequences (see Fig. 1A). In addition, BSSVS-BF results showed the most significant viral transmission routes for serotype O, where the most intense were represented from Turkey to Egypt, from Egypt to Indonesia and from Myanmar to Japan (BF>1038.7) (Fig. 3B).

Serotype O also showed the highest host diversity among all FMDV serotypes, which is represented by cattle (*Bos taurus*), swine (*Sus scrofa domesticus*), boar (*Sus scrofa*), sheep (*Ovis aries*), and the water buffalo (*Bubalus bubalis*), where the most representative were *B. taurus* (71% of the sequences) and *S. scrofa domesticus* (20%). *B. taurus* was not only the most important host for this serotype but also the most likely initial host of the ancestral lineages (RSPP= 0.95), followed by *S. scrofa domesticus* (RSPP= 0.03) and *O. aries* (RSPP= 0.032) respectively (Fig. 2). Bayes factor analysis showed that the most significant transmission routes occurred from *B. taurus* to *S. scrofa domesticus* (BF= 635.3), followed by from *B. taurus* to *O. aries* (BF=73.6), and in a minor scale, from *S. scrofa domesticus* to *B. taurus* (BF= 9.7), as well as from *B. taurus* to *B. bubalis* (BF=9.1) (Fig. 3C).

The Bayesian skyline plot (BSP) was used to describe the observed changes in genetic diversity (population size) through time, showing a steady pattern in this serotype, with a sharp decrease in its effective population size occurred ~2000, which returned to previous rates years later (Fig. S2).

Serotype A

Phylogeographic relationships obtained for serotype A indicated India as its most likely center of origin (RSPP= 0.28, Fig. 4). Besides, several centers of diversification have been identified for this serotype, where the most important have been India and Malaysia in Asia, Netherlands and Germany in Europe, Chad in Africa and Brazil in South America (Fig. 4). Our phylogeographic analysis also highlighted the importance of Brazil as a center of origin for a wide variety of European and South American lineages (Fig. 4). As in serotype O, we observed that long-distance dispersal events were the most representative of the spatiotemporal dynamics of this serotype, evidencing a global distribution, with records from 33 countries (Fig. 5B), which represents 33% of the total FMDV sequences.

BSSVS-BF analysis evidenced that the most significant transmission routes for this serotype come from India. Bayesian Factor analysis describing the most important viral transmission routes highlighted the importance of India in different directions, mainly to Netherlands (BF= 173.2), to Chad (BF= 162.9), and to Malaysia (BF= 28.3). Likewise, some European, such as Germany appeared to be important for the spread of this serotype into South America (BF=81.6, Fig. 5B).

The host species that showed highest number of serotype A sequences comes from *B. taurus* (82%), followed by *O. aries* (10%), *S. scrofa domesticus* (6%), and *B. bubalis* (2%) (Supplementary Table S1). Thus, the most important host behind the origin of the analyzed sequences of serotype A was *B. taurus* (RSPP= 0.98, Fig. 4). Furthermore, Bayes factor analysis indicated that the most significant transmission routes for the spread of this serotype occurred from *B. taurus* to all the other host. In order of significance, we can observe: to *S. scrofa domesticus* (BF= 1256.8), to *B. bubalis* (BF= 628.5), and to *O. aries* (BF= 74.1, Fig. 5C).

The BSP for this serotype showed a constant lineage diversity with a slight increase in 1980. The biggest variations between the years 2000 -2017, showed a sharp decrease followed by a rapid increase in lineage diversity that was maintained until 2010 when these values mostly returned to the original values (Fig. S2).

Serotype Asia1

This serotypes represented 12% of the entire FMDV sequences. Similarly to serotype A, phylogeographic analyses indicated India as the most likely origin of this serotype (RSPP= 0.34), from which it diverged in all directions (Fig. 6, Supplementary Video S3). The phylogenetic relationships seen in this serotype show a clear disparity between the lineages found in countries from western Asia (i.e., Israel, Lebanon, Afghanistan, and Turkey) and eastern Asia (i.e., China, Mongolia, Malaysia, and Vietnam) (Fig. 7A). Phylodynamic analysis shows that the most important centers of diversification for this serotype are India, China,

Pakistan and Vietnam (Fig. 7A). BSSVS-BF analysis showed similar results as the observed in serotype A, where the most significant transmission routes are related to India. In order of intensity, the most important routes are the ones from India to China (BF= 182.8) and from India to Vietnam (BF= 61.5) (Fig. 7B).

In relation to the number of available sequences, the most representative hosts for this serotype were *B. taurus* (66% of the sequences), followed by *S. scrofa* (14%, exclusively in China), *B. bubalis* (6%, observed in India, Vietnam, and China) and *O. aries* (~3%, observed only in China). Phylogenetic analysis showed that the hosts responsible for the spread of this serotype were *B. taurus* (RSPP= 0.98), followed by *S. scrofa* (RSPP= 0.2). In addition, Bayes factor analysis indicated that the most strongly supported transmission routes for the spread of this serotype occurred from *B. taurus* to *B. bubalis* (BF= 1405.6), followed by from *B. taurus* to *S. scrofa* (BF= 401.3), and from *B. taurus* to *O. aries* (BF= 134.1) (Fig. 7C).

Phylodynamic patterns of serotype Asia1 spread through BSP approach showed a constant lineage diversity over time, with a very slight variation around the year 2000 (Fig. S2).

Serotype SAT1

The phylogeographic patterns of SAT1 exposed Uganda as its most likely country of origin (RSPP= 0.45), from where it spread to Namibia, Nigeria, and Chad (Fig. 8). The phylogenetic relationships identified three main clusters, one of them represented by the ancestor of the lineages found in Uganda and Chad, other by the lineages located in the countries that are part of the southern area of spread (i.e., Botswana, Mozambique, Namibia, South Africa and Tanzania), and the last cluster represented by the lineages found in Nigeria, which also presented the sub-lineage with the most recent appearance. Contrary to the previous serotypes, SAT1 did not present a clear source (country) of dispersal events, although its spread was mostly concentrated on Eastern Africa (Fig. 9A). Our results showed that the highest proportion of its dispersal events occurred across long distance countries (representing 63% of the cases, See Supplementary Video S4 for detailed footage). The most significant dispersal routes were strongly related to Uganda, which in order of intensity, were seen to happen from Uganda to Nigeria (BF= 35.2), which seemed the most significant, followed by the transition from Kenya to Tanzania (BF= 26.5) (Fig. 9B).

The host species associated with the dispersal of this serotype were *B. taurus* and *S. caffer* (Fig. 8). *B. taurus*, with the majority of the number of sequences (58.3%), is mostly distributed in the north and central Africa, while *S. caffer* (41.7%, appeared as the most common host species in the southern countries (i.e., Namibia, Botswana, and South Africa). Phylogenetic analysis suggested *B. taurus* as the most important host species for the origin of this serotype (RSPP= 0.98). Strongly supported transmission routes were inferred from *B. taurus to S. caffer* (BF= 1233.3). However, the reverse transmission was not significant (BF<3) (Fig. 8).

Intriguingly, SAT1 BSP showed the most variable lineage diversity between all SATs, with an early increased in 1860 that was maintained until 1970, where this diversity increased again, reaching the values observed today (Fig. S2).

Serotype SAT2

Phylogeographic analyses for SAT2 indicated Uganda as the most likely origin of the serotype (RSPP= 0.51), from which it spread to Botswana and The Gaza Strip later on time (Fig. 10). Later, from Botswana, this serotype expanded its distribution to Ethiopia, Zimbabwe, and Zambia, continuing spreading to surrounding countries also on the Eastern region of Africa (see Supplementary Video S5 for detailed footage). Phylogenetic analysis identified two main sub-lineages, one found between Uganda and Gaza Strip and the second cluster formed by the lineages found in countries distributed in southeastern Africa (Fig. 10). Likewise, our results also evidenced that serotype SAT2 spread is mostly characterized by a higher proportion of long-distance movements (57%) over local dispersal events (Fig. 11A). Our phylodynamic model suggested that the strongest geographic transition routes occurred from Uganda to Gaza Strip (BF= 34.6), and from Botswana to Zambia (BF= 23.2) (Fig. 11B).

B. taurus and S. caffer were also the main host associated with SAT2 sequences, but in this case, *S. caffer* was the most representative (53.9%), over *B. taurus* (46.1%). However, *B. taurus* appeared in most of the reported locations (except in South Africa), while *S. caffer* was only described in Uganda, Botswana and South Africa. As observed in SAT1, phylogenetic analysis showed a higher influence of *B. taurus* as the host of the ancestral lineages of this serotype (RSPP= 0.63) (Fig. 10). Transmission dynamics between host species suggested that transmission from *B. taurus to S. caffer* was the most important (BF= 911.4), while transmission from *S. caffer* to *B. taurus* was not significant (BF<3) (Fig. 7D). Finally, BSP showed no variation in the lineage diversity found over time (Fig. S2).

Serotype SAT3

Similar to the previous SAT serotypes, SAT3 also had its ancestral origin in Uganda (RSPP= 0.49), from where it traveled to Zimbabwe and then spread to its neighboring countries (Fig. 12, see Supplementary Video S6). Phylogenetic analyses identified two main sub-lineages, one of them found in Uganda and the second (and most diverse), present in the countries that are part of southern Africa (i.e., Botswana, South Africa, Zambia, and Zimbabwe). Phylogeographic reconstruction reflected the importance of Zimbabwe for the spread of this serotype, being this country the most common center of origin for the diffusion of the disease to Zambia, Botswana and most recently to South Africa. Contrary to all the other serotypes (except for Asia1), spatiotemporal dynamics of serotype SAT3 showed that its spread has been dominated by local events (75%, Fig. 13A). Based on BSSVS-BF results, the most significant viral transmission routes for serotype SAT3 were represented by the dispersion from Zimbabwe to Botswana (BF= 15.9) and from Zimbabwe to South Africa (BF= 12.1) (Fig. 13B).

B. taurus and S. caffer were also the main hosts reported for SAT3, appearing both in a similar proportion (*B. taurus*= 62.5%, and *S. caffer*= 37.5%). Similarly to all the serotypes above mentioned, cattle was the likely ancestral host species for this serotype (RSPP= 0.94). Furthermore, we found that most significant transmission routes for its spread occurred from *B. taurus to S. caffer* (BF= 792.9), while the transmission in the opposite direction was not significant (Fig. 12).

Like in the case of SAT2, the BSP obtained for this serotype showed no variation in the lineage diversity over time (Fig. S2).

Discussion

This study revealed new insights about the evolutionary dynamics of the FMDV's global transmission dynamics at serotype level. The most likely country of origin for each serotype was identified, along with its historical spread characteristics, and divergence patterns across its historical dispersal. Finally, we assessed the impact of each host interaction in the spread of FMDV, providing a comprehensive characterization of transmission dynamics between host species.

Phylogeographic patterns of FMDV spread

Global patterns of FMDV spread were considerably asymmetric in its spatiotemporal arrangement, showing important variation among all serotypes, as previously observed by [50] and [79]. On the other hand, our results yielded discrepancies regarding the phylogenetic relationships of FMDV serotypes due to the disagreements observed in the cladistic characterization of FMDV serotypes (monophyletic or polyphyletic origin) [52]. [46] and [50] suggested that O, A, Asia1, C, and SAT3 were monophyletic, while SAT1 and SAT2 serotypes were polyphyletic. However, our results indicated the presence of only three monophyletic serotypes (O, A, and Asia1), whilst all SAT serotypes appeared to have multiple ancestral origins which can be related to multiple points of independent introduction of the virus.

Serotypes with global distribution (O and A)

Serotype O has shown a remarkable widespread distribution across the globe. In half of a century, this serotype reached almost all continents, causing dramatic economic losses [58, 80, 81]. Root state posterior probability analysis inferred Belgium as the most likely center of origin for this serotype, which, as a result of being responsible for the majority of outbreaks worldwide [82], we can observe multiple centers of diversification in most of the continents. Our phylogeographic analysis showed that this spread has been characterized by lineage dispersal events between distant regions (i.e. to regions not sharing international dry borders with the origin country), instead of dispersal events between neighboring countries, which may be one of the keys for its successful global spread. Bayesian skyline plot showed a severe decline in the genetic diversity around early 21^{th} century, this interesting pattern also observed by [50]. This decline and recover in the effective population size could be directly related to the increase in the FMDV outbreaks that occurred worldwide, which was followed by an intensive control and prevention strategies. The intense wave of outbreaks occurred during that period worldwide included countries such as, Argentina [83, 84], the United Kingdom [85, 86], Brazil [87], India [88], and Taiwan [89, 90]. As we observed in our phylogeographic visualization, there is strong evidence that most of these outbreaks were strongly interconnected [25, 91–93], evidencing local and long-distance spread of serotype.

One of the reasons for the success of the evolutionary diversification of this serotype may also be related to the diversity of hosts that it affects, which is the highest among all serotypes. Globally, *B. taurus* represented the most important host species for the spread of serotype O, while *S. scrofa* was mostly related to the spread of this serotype in southeastern Asia. Thus, phylodynamic analysis suggested that viral transition rate between these two livestock was the strongest reported between all the reported hosts.

Following the pandemic patterns showed by serotype O, the next large-scale potential of diffusion was exhibited by serotype A. Phylogeographic analysis suggested India as the most likely center of origin of the current circulating serotype A strains. Supporting previous studies [26, 60], we observed that India was also a key source of dispersal events for this serotype since most of the current strains are strongly related to India. Whole genome sequences of this serotype have been recorded in three continents, Asia, Africa, and South America, where it was reported as the causing agent of one of the biggest FMDV outbreaks, which occurred in Argentina in 2011, affecting a total of 2,126 herds [84]. It is important to note, that there is evidence of a posterior spread of these serotypes (O and A) to other countries, mainly in South America, since both of them are currently found in nearly every country of the continent [26, 82]. However, due to the lack of whole-genome data, we were unable to further assess this spread.

As expected, the main host affected by serotype A was *B. taurus*. This species had an important role in its viral spread [55], especially in this globalized era, where the continuous increase in livestock trading markets facilitates the spread of transboundary animal diseases [94]. Likewise, our phylodynamic analysis showed that the most intense host species transmission route occurred from *B. taurus* to *S. caffer*, and apparently, the reverse transmission is an infrequent event.

Asia1 and SAT serotypes

Whereas our results showed that serotypes O and A have spread worldwide, serotypes Asia1 and SATs remained non-pandemic and confined in their endemic regions [82, 95]. Since there is a lack of detailed sequences data available, especially for African countries, it is important to note that these results may vary with a better representation of the currently circulating virus, although they support what has been previously described [59, 78, 79, 82].

Undoubtedly, India has been historically considered as one of the most important countries for the spread and maintenance of FMDV, especially for serotypes A, and Asia1 [26, 56, 79, 82] Indeed, our phylogeographic analyses showed India as the most likely origin country for Asia1 serotype [26, 79]. The spread of this serotype was mainly restricted to Asia [53, 56, 78], and characterized by local movements across the neighboring countries surrounding India, China and Malaysia, where it is well known that free and unrestricted animal movements across country borders may play a key role in the spread of FMDV [56, 96]. We also observed India as a key center of dispersal for this serotype, which coincides with previously reported results [56]. The arrival of Asia1 into Turkey in 2013 represents one of the most recent and longer dispersal events reported for this serotype, which was directly related to an Indian sub-lineage of the virus [97]. Likewise, there have been sporadic incursions into other countries such as Greece in 1984 and 2000 [78], Malaysia in 1999 [31] or Turkey in 2017 [56], whose outbreaks seemed to be caused also by independent sub-lineages from the rest of the outbreaks observed in these regions.

Despite a previous study described multiple potential origins for SAT serotypes, (i.e., SAT1 in Zimbabwe and SAT2 in Kenya [48]), our root state posterior probability results suggested Uganda as the most likely origin for all of them. Likewise, our phylogeographic analysis also highlighted the importance of Uganda as a primary source of dispersal events to different countries, where the most strongly significant routes were found from Uganda to Nigeria (SAT1), from Uganda to Gaza strip (SAT2) and from Zimbabwe to Botswana (SAT3).

SAT serotypes (SAT1, SAT2, and SAT3) are characterized by a higher proportion of local spread, limited across their endemic areas. This spread occurred mainly in southeastern Africa, where nomadic pastoralism across international borders and animal trade in the sub-Saharan region is one of the most practiced forms of livestock movements [48, 55, 78, 79]. These results complement the observations made by [98], who highlighted how nomadism and transhumance play a key role in disease transmission, especially in African countries.

Previous studies have highlighted the importance of African buffalo (*Syncerus caffer*), hypothesizing that current FMDV genotypes may emerge in domesticated host species from viral reservoirs maintained by this species [49, 53, 59, 79, 99–105] However, the uncertainty over the involvement of African buffalo arose the need for deeper research to confirm its influence in livestock outbreaks [79] Our results coincide with the evidence mentioned in a recent study by [48], where cattle appeared as the most important host species for the spread of FMDV, while buffalo played a secondary role. This pattern was observed not only in SATs but in all serotypes studied.

In general, we observed considerable differences in the spatiotemporal dynamics exhibited by the different serotypes. Where the serotypes with global distribution (O and A) presented the most asymmetrical pattern in the annual genetic diversity in comparison with (SAT and Asia1 serotypes). Cattle was observed to play a key role in the historical spread of all serotypes of FMDV. Likewise, our phylodynamic analysis inferred that the transmission route from cattle to buffalo was the most highly supported, pattern that was also observed for all serotypes, independently of its spread potential.

Serotypes such as Asia1 and SATs presented local spread rates, mainly associated with cattle and sheep (with special importance of buffalo in the case of SATs serotypes) supporting previously described results [48, 79], while serotypes O and A showed long-distance spread, covering higher extensions of territory between each outbreak, which also confirms previously described information [59]. These serotypes presented the highest variety of susceptible hosts, although we speculate that the main reason for their successful long-distance spread relies mostly on the international movement of cattle and swine due to the intensive commerce between countries.

Finally, important limitations related to the use of whole genome relay in the lack of good global data, especially in African countries which remains endemically affected by five different serotypes, therefore some countries with known FMDV circulation are not part of this study. However, to reduce the bias generated by the strong unbalance of the available data in both dimensions (i.e., number of samples per country and uneven number of samples per host species), we removed all the sequences that where duplicated (i.e., represented the same outbreak multiple times), which, in the case of big outbreaks such as United Kingdom 2001/2007, Argentina 2001, and Japan 2010, accounted for hundreds of sequences representing each event. This limitation is common among phylogenic studies with no yet best alternative, this is true mainly because sample that are available hosted in public databases or from diagnostic laboratories [106]. Although whole genome sequences are increasingly proving to be a more accurate tool for phylogenetic analyses [107, 108], its high cost in comparison to studies considering partial genome results in lower availability of WGS, which became the major limitation for the construction of our dataset, resulting several countries with known reports of FMDV but lacking genetic data. Finally, it is important to highlight that, despite the nucleotide sequences encoding the capsid protein VP1, VP2, and VP3 are sufficient to identify FMDV at serotype level, WGS is preferred because of its higher accuracy in the determination of the genetic relationship between the reported cases [109].

Final remarks

Studies considering whole genome sequences should be preferred over partial sequence research to ensure the importance of considering virus spread in its overall context

[53, 107, 108]. Besides, the growing awareness of the importance of using whole genome sequences to assess the evolution of infectious diseases, and more specifically for RNA viruses as FMDV plays a key role on the future ability to analyze the ever-increasing volume of data accurately, getting closer to a real-time assessing of disease outbreaks [107]. However, the use of whole genome sequences represented a limitation in our study since the lack of FMDV sequences in a given country does not mean that the virus has not been circulating in that country but maybe associated with technical or economic constraints, therefore interpretation requires caution due to the possible introduction of sampling bias. The popularization of whole genome sequencing will help not only to increase the available information about the virus, but also have a direct impact on promoting new and more specific measures for disease control [24, 59, 110]. The result of such improvement in disease surveillance would not only be beneficial for the targeted region, but also for all the areas that are directly connected (i.e., through geographical limits) and indirectly (i.e., through commercial networks), including countries currently considered as free zones [111]. Even though past studies have found recombination in WGS of FMDV [53, 60], it is important to mention that after filtering the dataset to keep just one sequence per outbreak event, we did not found evidence of recombination on the remaining samples.

Conclusion

In summary, we have seen how FMDV evolved and diversified in five species among 64 countries, by using a comprehensive phylodynamic approach; we characterized and compared its global phylogeographic distribution at serotype scale. The phylogeographic approach used here relies on the principle that evolutionary processes are better understood when a broader spatiotemporal vision is available. Our results shed light on FMDV's macroevolutionary patterns and spread, allowing to unravel the ancestral country of origin for each serotype as well as the most important historical routes of viral dispersal, the role that the main host species played in its spatial diffusion and how likely the disease is transmitted between them. The use of whole genome sequences allowed us to clarify past discrepancies related to the polyphyletic nature of some serotypes (i.e., SATs), previously described as monophyletic.

Based on our findings, we corroborate with recent advancements that have been undertaken to control global distribution of major arbovirus (i.e., Dengue, yellow fever and Zika) [112–114], with the need to also implement real-time genome-scale sequencing to food-animal epidemics, in which metagenomics and phylogeography approaches inform epidemic responses and improve control intervention strategies.

Abbreviations

BSSVS: Bayesian stochastic search variable selection

BSP: Bayesian skyline plot

FMDV: Foot-and-mouth disease virus

MCMC: Markov chain Monte Carlo

TAD: transboundary animal disease

RDP: Recombination detection program

RSPP: Root state posterior probability

SAT: Southern African territories

WGS: Whole genome sequences

Declarations

Authors' Contributions

MJ contributed to the design of the project, the phylogeographic analyses, the visualization of the results, and wrote the manuscript. AF contributed to the data collection and curation, and wrote the manuscript. SD and GB contributed to the design of the methods and its supervision. GM contributed to the design of the project, supervised the methods and wrote the manuscript.

Acknowledgements

Not applicable

Funding

The Department of Population Health and Pathobiology- North Carolina State University provided startup funds for Dr. Machado and Dr. Jara and CVM for the intramural grant. Dr. Dellicour is supported by the Fonds National de la Recherche Scientifique (FNRS, Belgium). Dr. Baele acknowledges support from the Interne Fondsen KU Leuven / Internal Funds KU Leuven under grant agreement C14/18/094.

Availability of data and materials

All the sequences including country of origin, host and date are comes from Virus Pathogen Resource database, available at https://www.viprbrc.org. In addition, all the data used in this study is part of the supplementary material (See Table S1).

Competing interests

The authors declare that there is no conflict of interests.

Ethics approval and consent to participate

Not applicable.

Consent for publication

Not applicable.

References

1. Burrell A. Animal Disease Epidemics: Implications for Production, Policy and Trade. Outlook Agric. 2002;31:151–60. doi:10.5367/000000002101294001.
2. Otte MJ, Nugent R, McLeod A. Transboundary animal diseases: Assessment of socio-economic impacts and institutional responses. In: Food and Agriculture Organization (FAO). 2004. p. 119–26.
3. Daszak P, Cunningham AA, Hyatt AD. Anthropogenic environmental change and the emergence of infectious diseases in wildlife. Acta Trop. 2001;78:103–16. https://www.sciencedirect.com/science/article/pii/S0001706X00001790. Accessed 12 Oct 2018.

4. Kouba V. Globalization of Communicable Animal Diseases - A Crisis of Veterinary Medicine. Acta Vet Brno. 2003;72:453–60. doi:10.2754/avb200372030453.
5. Smith KF, Sax DF, Gaines SD, Guernier V, Guégan JF. Globalization of human infectious disease. Ecology. 2007;88:1903–10. doi:10.1890/06-1052.1.
6. Kilpatrick AM. Globalization, land use, and the invasion of West Nile virus. Science. 2011;334:323–7. doi:10.1126/science.1201010.
7. Wang T, Sun Y, Qiu H-J. African swine fever: an unprecedented disaster and challenge to China. Infect Dis poverty. 2018;7:111. doi:10.1186/s40249-018-0495-3.
8. Stearns SC, Ebert D. Evolution in Health and Disease: Work in Progress. Q Rev Biol. 2001;76:417–32. doi:10.1086/420539.
9. Read AF, Aaby P, Antia R, Ebert D, Ewald PW, Gupta S, et al. What can evolutionary biology contribute to understanding virulence? In: Evolution in Health and Disease. 1999. p. 205–16. http://www.evolution.unibas.ch/ebert/publications/papers/03_book_chapters/1999_Read_in_StearnsBOOK.PDF. Accessed 15 Jan 2019.
10. Trevathan W. Evolutionary medicine. In: The International Encyclopedia of Biological Anthropology. Hoboken, NJ, USA: John Wiley & Sons, Inc.; 1999. p. 1–4. doi:10.1002/9781118584538.ieba0534.
11. Galvani AP. Epidemiology meets evolutionary ecology. Trends in Ecology and Evolution. 2003;18:132–9. doi:10.1016/S0169-5347(02)00050-2.
12. Mideo N, Alizon S, Day T. Linking within- and between-host dynamics in the evolutionary epidemiology of infectious diseases. Trends in Ecology and Evolution. 2008;23:511–7. doi:10.1016/j.tree.2008.05.009.
13. Lion S, Gandon S. Spatial evolutionary epidemiology of spreading epidemics. Proc R Soc B Biol Sci. 2016;283. doi:10.1098/rspb.2016.1170.
14. Magiorkinis G, Magiorkinis E, Paraskevis D, Ho SYW, Shapiro B, Pybus OG, et al. The global spread of hepatitis C virus 1a and 1b: A phylodynamic and phylogeographic analysis. PLoS Med. 2009;6:e1000198. doi:10.1371/journal.pmed.1000198.
15. Weaver SC, Forrester NL. Chikungunya: Evolutionary history and recent epidemic spread. Antiviral Res. 2015;120:32–9. doi:10.1016/j.antiviral.2015.04.016.
16. Dellicour S, Lemey P, Rose R, Faria NR, Pybus OG, Vieira LFP, et al. Using Viral Gene Sequences to Compare and Explain the Heterogeneous Spatial Dynamics of Virus Epidemics. Mol Biol Evol. 2017;34:2563–71. https://academic.oup.com/mbe/article-abstract/34/10/2563/3885213. Accessed 15 Jan 2019.
17. Forni D, Cagliani R, Clerici M, Sironi M. Origin and dispersal of Hepatitis e virus article. Emerg Microbes Infect. 2018;7. doi:10.1038/s41426-017-0009-6.
18. Stephens PR, Altizer S, Smith KF, Alonso Aguirre A, Brown JH, Budischak SA, et al. The macroecology of infectious diseases: a new perspective on global-scale drivers of pathogen distributions and impacts. Ecol Lett. 2016;19:1159–71. doi:10.1111/ele.12644.
19. Jacquot M, Nomikou K, Palmarini M, Mertens P, Biek R. Bluetongue virus spread in Europe is a consequence of climatic, landscape and vertebrate host factors as revealed by phylogeographic inference. Proc R Soc B Biol Sci. 2017;284. doi:10.1098/rspb.2017.0919.
20. Lemey P, Pybus OG, Holmes EC, Grubaugh ND, Ladner JT, Rambaut A, et al. Tracking virus outbreaks in the twenty-first century. Nat Microbiol. 2018;4:10–9. doi:10.1038/s41564-018-0296-2.
21. Auguste AJ, Liria J, Forrester NL, Giambalvo D, Moncada M, Long KC, et al. Evolutionary and ecological characterization of mayaro virus strains isolated during an outbreak, Venezuela, 2010. Emerg Infect Dis. 2015;21:1742–50. doi:10.3201/eid2110.141660.
22. Pigeault R, Vézilier J, Cornet S, Zélé F, Nicot A, Perret P, et al. Avian malaria: A new lease of life for an old experimental model to study the evolutionary ecology of Plasmodium. Philos Trans R Soc B Biol Sci. 2015;370. doi:10.1098/rstb.2014.0300.
23. Rogalski MA, Gowler CD, Shaw CL, Hufbauer RA, Duffy MA. Human drivers of ecological and evolutionary dynamics in emerging and disappearing infectious disease systems. Philosophical Transactions of the Royal Society B: Biological Sciences. 2017;372. doi:10.1098/rstb.2016.0043.
24. Fountain-Jones NM, Pearse WD, Escobar LE, Alba-Casals A, Carver S, Davies TJ, et al. Towards an eco-phylogenetic framework for infectious disease ecology. Biol Rev. 2018;93:950–70. doi:10.1111/brv.12380.
25. Grubman MJ, Baxt B. Foot-and-mouth Disease. Clin Microbiol Rev. 2004;17:465–93. http://cmr.asm.org/content/17/2/465.short. Accessed 12 Oct 2018.
26. Brito B, Perez AM, Mohapatra J, Subramaniam S, Pattnaik B, Rodriguez LL, et al. Dynamics of widespread foot-and-mouth disease virus serotypes A, O and Asia-1 in southern Asia: A Bayesian phylogenetic perspective. Transbound Emerg Dis. 2017;65:696–710. https://onlinelibrary.wiley.com/doi/abs/10.1111/tbed.12791. Accessed 14 Apr 2019.
27. Belsham G. Distinctive features of foot-and-mouth disease virus, a member of the picornavirus family; aspects of virus protein synthesis, protein processing and structure. Prog Biophys Mol Biol. 1993;60:241–60. https://www.sciencedirect.com/science/article/pii/007961079390016D. Accessed 15 Jan 2019.
28. Sobrino F, Sáiz M, Jiménez-Clavero MA, Núñez JI, Rosas MF, Baranowski E, et al. Foot-and-mouth disease virus: A long known virus, but a current threat. Veterinary Research. 2001;32:1–30. doi:10.1051/vetres:2001106.
29. Brown F. The history of research in foot-and-mouth disease. Virus Res. 2003;91:3–7. https://www.sciencedirect.com/science/article/pii/S016817020200268X. Accessed 3 Oct 2018.
30. OIE TM. Foot-And-Mouth Disease. 2009. doi:10.1146/annurev.mi.22.100168.001221.
31. Abdul-Hamid NF, Hussein NM, Wadsworth J, Radford AD, Knowles NJ, King DP. Phylogeography of foot-and-mouth disease virus types O and A in Malaysia and surrounding countries. Infect Genet Evol. 2011;11:320–8. doi:10.1016/j.meegid.2010.11.003.
32. Kandeil A, El-Shesheny R, Kayali G, Moatasim Y, Bagato O, Darwish M, et al. Characterization of the recent outbreak of foot-and-mouth disease virus serotype SAT2 in Egypt. Arch Virol. 2013;158:619–27. doi:10.1007/s00705-012-1529-y.

33. Ganji V, Kontham S, Pottabathula M. Understanding the Molecular Relationship between Foot-and-Mouth Disease Virus Serotype O of Indian Vaccine Strain with Strains across the World by. Phylogenetic Anal Int J Curr Microbiol. 2018;7:99–105. https://www.ijcmas.com/7-5-2018/Vishweshwar Kumar Ganji, et al.pdf. Accessed 18 Oct 2018.
34. Knight-Jones T, Rushton J. The economic impacts of foot and mouth disease - What are they, how big are they and where do they occur? Preventive Veterinary Medicine. 2013;112:162–73. doi:10.1016/j.prevetmed.2013.07.013.
35. Alvarez J, Goede D, Morrison R, Perez A. Spatial and temporal epidemiology of porcine epidemic diarrhea (PED) in the Midwest and Southeast regions of the United States. Prev Vet Med. 2016;123:155–60. doi:10.1016/j.prevetmed.2015.11.003.
36. Rushton J, Knight-Jones TJD. The impact of foot and mouth disease. In: FAO/OIE, Global Conference on Foot and Mouth Disease Control. Food and Agriculture Organization of the United Nations and the World Organisation for Animal Health; 2015. p. 205–9. doi:10.1111/j.1746-692X.2004.tb00031.x.
37. USDA-APHIS. Planning and preparing for Foot-and-mouth disease: quick briefing. 2017. https://www.aphis.usda.gov/animal_health/emergency_management/downloads/fmd-briefing.pdf.
38. Alexandersen S, Zhang Z, Donaldson AI, Garland AJM. The pathogenesis and diagnosis of foot-and-mouth disease. Journal of Comparative Pathology. 2003;129:1–36. doi:10.1016/S0021-9975(03)00041-0.
39. IUCN/SSC ISSG. Global Invasive Species Database version 2013-1. 2018. http://www.issg.org/database/welcome/. Accessed 14 Oct 2018.
40. Thomson GR, Bastos A. Foot-and-mouth disease. In: Infectious Diseases of Livestock. Cape Town: Oxford University Press; 2004. p. 1324–65.
41. Orsel K, Bouma A, Dekker A, Stegeman JA, de Jong MCM. Foot and mouth disease virus transmission during the incubation period of the disease in piglets, lambs, calves, and dairy cows. Prev Vet Med. 2009;88:158–63. doi:10.1016/j.prevetmed.2008.09.001.
42. Ferguson NM, Donnelly CA, Anderson RM. Transmission intensity and impact of control policies on the foot and mouth epidemic in Great Britain. Nature. 2001;413:542–8. https://www.nature.com/articles/35097116. Accessed 15 Jan 2019.
43. Fares M a, Tully DC. The tale of a modern animal plague: tracing the evolutionary history and determining the time-scale for foot and mouth disease virus. Virology. 2008;382:250–6. doi:10.1016/j.virol.2008.09.011.
44. Schumann KR, Knowles NJ, Davies PR, Midgley RJ, Valarcher J-F, Raoufi AQ, et al. Genetic characterization and molecular epidemiology of foot-and-mouth disease viruses isolated from Afghanistan in 2003–2005. Virus Genes. 2008;36:401–13. doi:10.1007/s11262-008-0206-4.
45. Priyadarshini P, Mohapatra JK, Hemadri D, Subramaniam S, Pattnaik B, Pandey L, et al. Analysis of the leader proteinase (Lpro) region of type A foot-and-mouth disease virus with due emphasis on phylogeny and evolution of the emerging VP359-deletion lineage from India. Virus Res. 2009;141:34–46. doi:10.1016/j.virusres.2008.12.012.
46. Lewis-Rogers N, McClellan DA, Crandall KA. The evolution of foot-and-mouth disease virus: Impacts of recombination and selection. Infect Genet Evol. 2008;8:786–98. doi:10.1016/j.meegid.2008.07.009.
47. Lycett SJ, Tanya VN, Hall M, King D, Mazeri S, Mioulet V, et al. The evolution and phylodynamics of serotype A and SAT2 foot-and-mouth disease viruses in endemic regions of Africa. Sci Rep. 2019;9:5614. doi:10.1101/572198.
48. Omondi G, Alkhamis MA, Obanda V, Gakuya F, Sangula A, Pauszek S, et al. Phylogeographical and cross-species transmission dynamics of SAT1 and SAT2 foot-and-mouth disease virus in Eastern Africa. Mol Ecol. 2019;:mec.15125. doi:10.1111/mec.15125.
49. Hall MD, Knowles NJ, Wadsworth J, Rambaut A, Woolhouse MEJ. Reconstructing geographical movements and host species transitions of foot-and-mouth disease virus serotype SAT 2. MBio. 2013;4:e00591-13. doi:10.1128/mBio.00591-13.
50. Yoon SH, Park W, King DP, Kim H. Phylogenomics and molecular evolution of foot-and-mouth disease virus. Mol Cells. 2011;31:413–21. doi:10.1007/s10059-011-0249-6.
51. Carrillo C, Tulman ER, Delhon G, Lu Z, Carreno A, Vagnozzi A, et al. Comparative genomics of foot-and-mouth disease virus. J Virol. 2005;79:6487–504. doi:10.1128/JVI.79.10.6487-6504.2005.
52. Cooke JN, Westover KM. Serotype-specific differences in antigenic regions of foot-and-mouth disease virus (FMDV): A comprehensive statistical analysis. Infect Genet Evol. 2008;8:855–63. doi:10.1016/j.meegid.2008.08.004.
53. Lasecka-Dykes L, Wright CF, Di Nardo A, Logan G, Mioulet V, Jackson T, et al. Full genome sequencing reveals new southern african territories genotypes bringing us closer to understanding true variability of foot-and-mouth disease virus in Africa. Viruses. 2018;10. doi:10.3390/v10040192.
54. Baele G, Dellicour S, Suchard MA, Lemey P, Vrancken B. Recent advances in computational phylodynamics. Curr Opin Virol. 2018;31:24–32. doi:10.1016/J.COVIRO.2018.08.009.
55. Di Nardo. A, Knowles N, Paton D. Combining livestock trade patterns with phylogenetics to help understand the spread of foot and mouth disease in sub-Saharan Africa, the Middle East and. Rev Sci Tech. 2011;30:63. http://www.unitheque.com/UploadFile/DocumentPDF/L/A/OMMT-9789290448372.pdf. Accessed 15 Jan 2019.
56. Brito B, Pauszek SJ, Eschbaumer M, Stenfeldt C, De Carvalho Ferreira HC, Vu LT, et al. Phylodynamics of foot-and-mouth disease virus O/PanAsia in Vietnam 2010-2014. Vet Res. 2017;48:24. doi:10.1186/s13567-017-0424-7.
57. De Carvalho LMF, Santos LBL, Faria NR, De Castro Silveira W. Phylogeography of foot-and-mouth disease virus serotype O in Ecuador. Infect Genet Evol. 2013;13:76–88. doi:10.1016/j.meegid.2012.08.016.
58. Bachanek-Bankowska K, Di Nardo A, Wadsworth J, Mioulet V, Pezzoni G, Grazioli S, et al. Reconstructing the evolutionary history of pandemic foot-and-mouth disease viruses: the impact of recombination within the emerging O/ME-SA/Ind-2001 lineage. Sci Rep. 2018;8:14693. doi:10.1038/s41598-018-32693-8.
59. Duchatel F, Bronsvoort M, Lycett S. Phylogeographic analysis and identification of factors impacting the diffusion of Foot-and-Mouth disease virus in Africa. Front Ecol Evol. 2019;7:371.

60. Brito B, Pauszek SJ, Hartwig EJ, Smoliga GR, Vu LT, Dong P V., et al. A traditional evolutionary history of foot-and-mouth disease viruses in Southeast Asia challenged by analyses of non-structural protein coding sequences. Sci Rep. 2018;8. doi:10.1038/s41598-018-24870-6.
61. Kumar S, Nei M, Dudley J, Tamura K. MEGA: A biologist-centric software for evolutionary analysis of DNA and protein sequences. Brief Bioinform. 2008;9:299–306. doi:10.1093/bib/bbn017.
62. Martin DP, Murrell B, Golden M, Khoosal A, Muhire B. RDP4: Detection and analysis of recombination patterns in virus genomes. Virus Evol. 2015;1. doi:10.1093/ve/vev003.
63. Rambaut A, Lam T, Max Carvalho L, Pybus O. Exploring the temporal structure of heterochronous sequences using TempEst (formerly Path-O-Gen). Virus Evol. 2016;2:vew007. doi:10.1093/ve/vew007.
64. Murray GGR, Wang F, Harrison EM, Paterson GK, Mather AE, Harris SR, et al. The effect of genetic structure on molecular dating and tests for temporal signal. Methods Ecol Evol. 2016;7:80–9. doi:10.1111/2041-210X.12466.
65. Navascués M, Depaulis F, Emerson B. Combining contemporary and ancient DNA in population genetic and phylogeographical studies. Mol Ecol Resour. 2010;10:760–72. doi:10.1111/j.1755-0998.2010.02895.x.
66. Bouckaert R, Heled J, Kühnert D, Vaughan T, Wu CH, Xie D, et al. BEAST 2: A Software Platform for Bayesian Evolutionary Analysis. PLoS Comput Biol. 2014;10:e1003537. doi:10.1371/journal.pcbi.1003537.
67. Hasegawa M, Kishino H, Yano T. Dating of the human-ape splitting by a molecular clock of mitochondrial DNA. J Mol Evol. 1985;22:160–74. doi:10.1007/BF02101694.
68. Shapiro B, Rambaut A, Drummond AJ. Choosing appropriate substitution models for the phylogenetic analysis of protein-coding sequences. academic.oup.com. 2006;23:7–9. doi:10.1093/molbev/msj021.
69. Russel PM, Brewer BJ, Klaere S, Bouckaert RR. Model Selection and Parameter Inference in Phylogenetics Using Nested Sampling. Syst Biol. 2019;68:219–33. doi:10.1093/sysbio/syy050.
70. Drummond AJ, Ho SYW, Phillips MJ, Rambaut A. Relaxed phylogenetics and dating with confidence. PLoS Biol. 2006;4:e88. doi:10.1371/journal.pbio.0040088.
71. Drummond A, Rambaut A, Shapiro B, Pybus OG. Bayesian coalescent inference of past population dynamics from molecular sequences. Mol Biol Evol. 2005;22:1185–92. doi:10.1093/molbev/msi103.
72. Rambaut AR, Drummond ALJ, Dong X, Baele G, Suchard M. Posterior Summarization in Bayesian Phylogenetics Using Tracer 1 . 7. Syst Biol. 2018;67:901–4. doi:10.1093/sysbio/syy032.
73. Rambaut A. FigTree-version 1.4. 3, a graphical viewer of phylogenetic trees. 2017.
74. Lemey P, Rambaut A, Drummond AJ, Suchard MA. Bayesian Phylogeography Finds Its Roots. PLoS Comput Biol. 2009;5:e1000520. doi:10.1371/journal.pcbi.1000520.
75. Drummond AJ, Bouckaert RR. Bayesian evolutionary analysis with BEAST. Cambridge University Press; 2015.
76. Bielejec F, Baele G, Vrancken B, Suchard M, Rambaut A, Lemey P. SpreaD3: interactive visualization of spatiotemporal history and trait evolutionary processes. Mol Biol Evol. 2016;33:2167–9. https://academic.oup.com/mbe/article-abstract/33/8/2167/2579258. Accessed 15 Jan 2019.
77. Fèvre E, Bronsvoort B, Hamilton K, Cleaveland S. Animal movements and the spread of infectious diseases. Trends in Microbiology. 2006;14:125–31. doi:10.1016/j.tim.2006.01.004.
78. Jamal SM, Belsham GJ. Foot-and-mouth disease: past, present and future. Vet Res. 2013;44:116. doi:10.1186/1297-9716-44-116.
79. Brito B, Rodriguez L, Hammond J, Pinto J, Perez A. Review of the Global Distribution of Foot-and-Mouth Disease Virus from 2007 to 2014. Transboundary and Emerging Diseases. 2015;64:316–32. doi:10.1111/tbed.12373.
80. Hemadri D, Tosh C, Sanyal A, Venkataramanan R. Emergence of a new strain of type O Foot-and-mouth disease virus: Its phylogenetic and evolutionary relationship with the PanAsia pandemic strain. Virus Genes. 2002;25:23–34. doi:10.1023/A:1020165923805.
81. Knowles NJ, Samuel AR, Davies PR, Midgley RJ, Valarcher J-F. Pandemic strain of foot-and-mouth disease virus serotype O. Emerg Infect Dis. 2005;11:1887–93. doi:10.3201/eid1112.050908.
82. Rweyemamu M, Roeder P, Mackay D, Sumption K, Brownlie J, Leforban Y, et al. Epidemiological Patterns of Foot-and-Mouth Disease Worldwide. Transbound Emerg Dis. 2008;55:57–72. doi:10.1111/j.1865-1682.2007.01013.x.
83. Perez AM, Ward MP, Carpenter TE. Control of a foot-and-mouth disease epidemic in Argentina. Prev Vet Med. 2004;65:217–26.
84. Perez AM, Ward MP, Carpenter TE. Epidemiological investigations of the 2001 foot-and-mouth disease outbreak in Argentina. Vet Rec. 2004;154:777–82. https://veterinaryrecord.bmj.com/content/154/25/777.short. Accessed 8 Mar 2019.
85. Thompson D, Muriel P, Russell D, Osborne P, Bromley A, Rowland M, et al. Economic costs of the foot and mouth disease outbreak in the United Kingdom in 2001. Rev Sci Tech. 2002;21:675–87. https://europepmc.org/abstract/med/12523706. Accessed 15 Jan 2019.
86. Gloster J, Paton DJ, Hutchings GH, King DP, Ferris NP, Haydon DT, et al. Molecular Epidemiology of the Foot-and-Mouth Disease Virus Outbreak in the United Kingdom in 2001. J Virol. 2006;80:11274–82. doi:10.1128/jvi.01236-06.
87. Melo EC, Saraiva V, Studillo V. Review of the status of foot and mouth disease in countries of South America and approaches to control and eradication. Rev Sci Tech Int des épizooties. 2002;21:429–33. doi:10.20506/rst.21.3.1350.
88. Huang CC, Lin YL, Huang TS, Tu WJ, Lee SH, Jong MH, et al. Molecular characterization of foot-and-mouth disease virus isolated from ruminants in Taiwan in 1999-2000. Vet Microbiol. 2001;81:193–205. doi:10.1016/S0378-1135(01)00308-X.

89. Dunn CS, Donaldson AI. Natural adaption to pigs of a Taiwanese isolate of foot-and-mouth disease virus. Vet Rec. 1997;141:174–5. doi:10.1136/vr.141.7.174.
90. Yang PC, Chu RM, Chung WB, Sung HT. Epidemiological characteristics and financial costs of the 1997 foot-and-mouth disease epidemic in Taiwan. Vet Rec. 1999;145:731–4. https://veterinaryrecord.bmj.com/content/145/25/731.short. Accessed 12 Jul 2019.
91. Knowles NJ, Samuel AR, Davies PR, Kitching RP, Donaldson AI. Outbreak of foot-and-mouth disease virus serotype O in the UK caused by a pandemic strain. Vet Rec. 2001;148:258–9. http://www.ncbi.nlm.nih.gov/pubmed/11292084. Accessed 12 Jul 2019.
92. Sangare O, Bastos AD, Marquardt O, Venter EH, Vosloo W, Thomson GR. Molecular epidemiology of serotype O foot-and-mouth disease virus with emphasis on West and South Africa. Virus Genes. 2001;22:345–51. https://link.springer.com/article/10.1023/A:1011178626292. Accessed 12 Jul 2019.
93. Pluimers FH, Akkerman AM, van der Wal P, Dekker A, Bianchi A. Lessons from the foot and mouth disease outbreak in The Netherlands in 2001. Rev Sci Tech. 2002;21:711–21. https://pdfs.semanticscholar.org/ada9/a1b0ecd88ea85df19e53b462fd897bff4b11.pdf. Accessed 12 Jul 2019.
94. Cartín-Rojas A. Transboundary animal diseases and international trade. In: International Trade from Economic and Policy Perspective. 2012. p. 143–66. https://books.google.com/books?hl=es&lr=&id=AO6dDwAAQBAJ&oi=fnd&pg=PA143&dq=Transboundary+animal+diseases+and+international+trade&ots=EFgRQFP16_&sig=7zwlV71w7VM Accessed 12 Jul 2019.
95. Kitching RP. Global Epidemiology and Prospects for Control of Foot-and-Mouth Disease. In: Foot-and-Mouth-Disease Virus. Heidelberg, Berlin: Springer-Verlag; 2005. p. 133–48. https://link.springer.com/content/pdf/10.1007/3-540-27109-0_6.pdf. Accessed 12 Jul 2019.
96. Subramaniam S, Pattnaik B, Sanyal A, Mohapatra JK, Pawar SS, Sharma GK, et al. Status of Foot-and-mouth Disease in India. Transbound Emerg Dis. 2013;60:197–203. doi:10.1111/j.1865-1682.2012.01332.x.
97. Upadhyaya S, Ayelet G, Paul G, King DP, Paton DJ, Mahapatra M. Genetic basis of antigenic variation in foot-and-mouth disease serotype A viruses from the Middle East. Vaccine. 2014;32:631–8. doi:10.1016/j.vaccine.2013.08.102.
98. Bouslikhane M. Cross border movements of animals and animal products and their relevance to the epidemiology of animals disease in Africa. OIE Africa Regional Commision.; 2015. https://pdfs.semanticscholar.org/3502/9521c392e33c47c1d7c039f9a172fc132008.pdf. Accessed 21 Mar 2019.
99. Dion E, VanSchalkwyk L, Lambin EF. The landscape epidemiology of foot-and-mouth disease in South Africa: A spatially explicit multi-agent simulation. Ecol Modell. 2011;222:2059–72. doi:10.1016/j.ecolmodel.2011.03.026.
100. Vosloo W, Bastos AD, Kirkbride E, Esterhuysen JJ, van Rensburg DJ, Bengis RG, et al. Persistent infection of African buffalo (Syncerus caffer) with SAT-type foot-and-mouth disease viruses: rate of fixation of mutations, antigenic change and interspecies transmission. J Gen Virol. 1996;77:1457–67. doi:10.1099/0022-1317-77-7-1457.
101. Thomson GR, Vosloo W, Bastos AD. Foot and mouth disease in wildlife. Virus Res. 2003;91:145–61. doi:10.1016/s0168-1702(02)00263-0.
102. Michel AL, Bengis RG. The Afican buffalo: A villain for inter-species spread of infectious diseases in southern Africa. OpenJournals Publishing; 2012. http://www.scielo.org.za/scielo.php?script=sci_arttext&pid=S0030-24652012000200006. Accessed 5 Jul 2019.
103. Bronsvoort BMDC, Parida S, Handel I, McFarland S, Fleming L, Hamblin P, et al. Serological survey for foot-and-mouth disease virus in wildlife in eastern Africa and estimation of test parameters of a nonstructural protein enzyme-linked immunosorbent assay for buffalo. Clin Vaccine Immunol. 2008;15:1003–11. doi:10.1128/CVI.00409-07.
104. Ayebazibwe C, Mwiine FN, Tjørnehøj K, Balinda SN, Muwanika VB, Ademun Okurut AR, et al. The role of African buffalos (syncerus caffer) in the maintenance of foot-and-mouth disease in Uganda. BMC Vet Res. 2010;6:54. doi:10.1186/1746-6148-6-54.
105. Dhikusooka MT, Tjørnehøj K, Ayebazibwe C, Namatovu A, Ruhweza S, Siegismund HR, et al. Foot-and-mouth disease virus serotype SAT 3 in long-horned ankole Calf, Uganda. Emerg Infect Dis. 2015;21:111–4. doi:10.3201/eid2101.140995.
106. Frost SDW, Pybus OG, Gog JR, Viboud C, Bonhoeffer S, Bedford T. Eight challenges in phylodynamic inference. Epidemics. 2015;10:88–92. doi:10.1016/j.epidem.2014.09.001.
107. Dudas G, Bedford T. The ability of single genes vs full genomes to resolve time and space in outbreak analysis. BiorXiv. 2019;:27. doi:10.1101/582957.
108. Gilchrist CA, Turner SD, Riley MF, Petri WA, Hewlett EL. Whole-genome sequencing in outbreak analysis. Clin Microbiol Rev. 2015;28:541–63. doi:10.1128/CMR.00075-13.
109. Mason PW, Pacheco JM, Zhao QZ, Knowles NJ. Comparisons of the complete genomes of Asian, African and European isolates of a recent foot-and-mouth disease virus type O pandemic strain (PanAsia). J Gen Virol. 2003;84:1583–93. doi:10.1099/vir.0.18669-0.
110. Schrag SJ, Wiener P. Emerging infectious disease: what are the relative roles of ecology and evolution. Trends Ecol Evol. 1995;10:319–24. https://www.sciencedirect.com/science/article/pii/S0169534700891181. Accessed 17 Jan 2019.
111. King D, Di Nardo A, Henstock M. OIE/FAO Foot-and-Mouth Disease Reference Laboratory Network: Annual report 2017. 2016;:91.
112. Thézé J, Li T, du Plessis L, Bouquet J, Kraemer MU, Somasekar S, et al. Genomic Epidemiology Reconstructs the Introduction and Spread of Zika Virus in Central America and Mexico. Cell host Microbe. 2018;23:1–10. https://www.sciencedirect.com/science/article/pii/S193131281830218X. Accessed 12 Jul 2019.
113. Faria NR, Kraemer MU, Hill S, De Jesus JG, De Aguiar RS, Iani FC, et al. Genomic and epidemiological monitoring of yellow fever virus transmission potential. BiorXiv. 2018.
114. Messina J, Brady O, Golding N, Kraemer MUG, Wint GRW, Ray SE, et al. The current and future global distribution and population at risk of dengue. Nat Microbiol. 2019;in press. https://www.nature.com/articles/s41564-019-0476-8. Accessed 12 Jul 2019.

Supplementary Material

Table S1. Sample information for all Foot and Mouth Disease virus complete genome sequences used in this study.

Table S2. Number of sequences and serotypes per country.

TABLE S3. Root-to-tip regression analyses of phylogenetic temporal signal. Correlation and determination coefficient (R2) were estimated with TempEst [63]. P-values were calculated using the approach of [64] and were based on 1,000 random permutations of the sequence sampling dates [65].

Fig. S1 Spatial distribution of Foot-and-mouth disease virus showing the number of serotypes per country.

Fig. S2 Reconstructed Bayesian Coalescent Skyline plots (BSP) of FMDV serotypes. The median estimated of the effective population size through time are represented by the dark blue. The 95% highest posterior density confidence intervals are marked in blue.

Video S1. Reconstructed spatiotemporal diffusion of FMD serotype O spread, where diameters of the colored circles are proportional to the square root of the number of MCC branches, maintaining a particular location state at each time period. The color of the branches represents the age of the internal nodes, where darker red colors represent older spread events, this visualization match with the main time bar on top of the video.

Video S2. Reconstructed spatiotemporal diffusion of FMD serotype A spread, where diameters of the colored circles are proportional to the square root of the number of MCC branches, maintaining a particular location state at each time period. The color of the branches represents the age of the internal nodes, where darker red colors represent older spread events, this visualization match with the main time bar on top of the video.

Video S3. Reconstructed spatiotemporal diffusion of FMD serotype Asia1 spread, where diameters of the colored circles are proportional to the square root of the number of MCC branches, maintaining a particular location state at each time period. The color of the branches represents the age of the internal nodes, where darker red colors represent older spread events, this visualization match with the main time bar on top of the video.

Video S4. Reconstructed spatiotemporal diffusion of FMD serotype SAT1 spread, where diameters of the colored circles are proportional to the square root of the number of MCC branches, maintaining a particular location state at each time period. The color of the branches represents the age of the internal nodes, where darker red colors represent older spread events, this visualization match with the main time bar on top of the video.

Video S5. Reconstructed spatiotemporal diffusion of FMD serotype SAT2 spread, where diameters of the colored circles are proportional to the square root of the number of MCC branches, maintaining a particular location state at each time period. The color of the branches represents the age of the internal nodes, where darker red colors represent older spread events, this visualization match with the main time bar on top of the video.

Video S6. Reconstructed spatiotemporal diffusion of FMD serotype SAT3 spread, where diameters of the colored circles are proportional to the square root of the number of MCC branches, maintaining a particular location state at each time period. The color of the branches represents the age of the internal nodes, where darker red colors represent older spread events, this visualization match with the main time bar on top of the video.

Figures

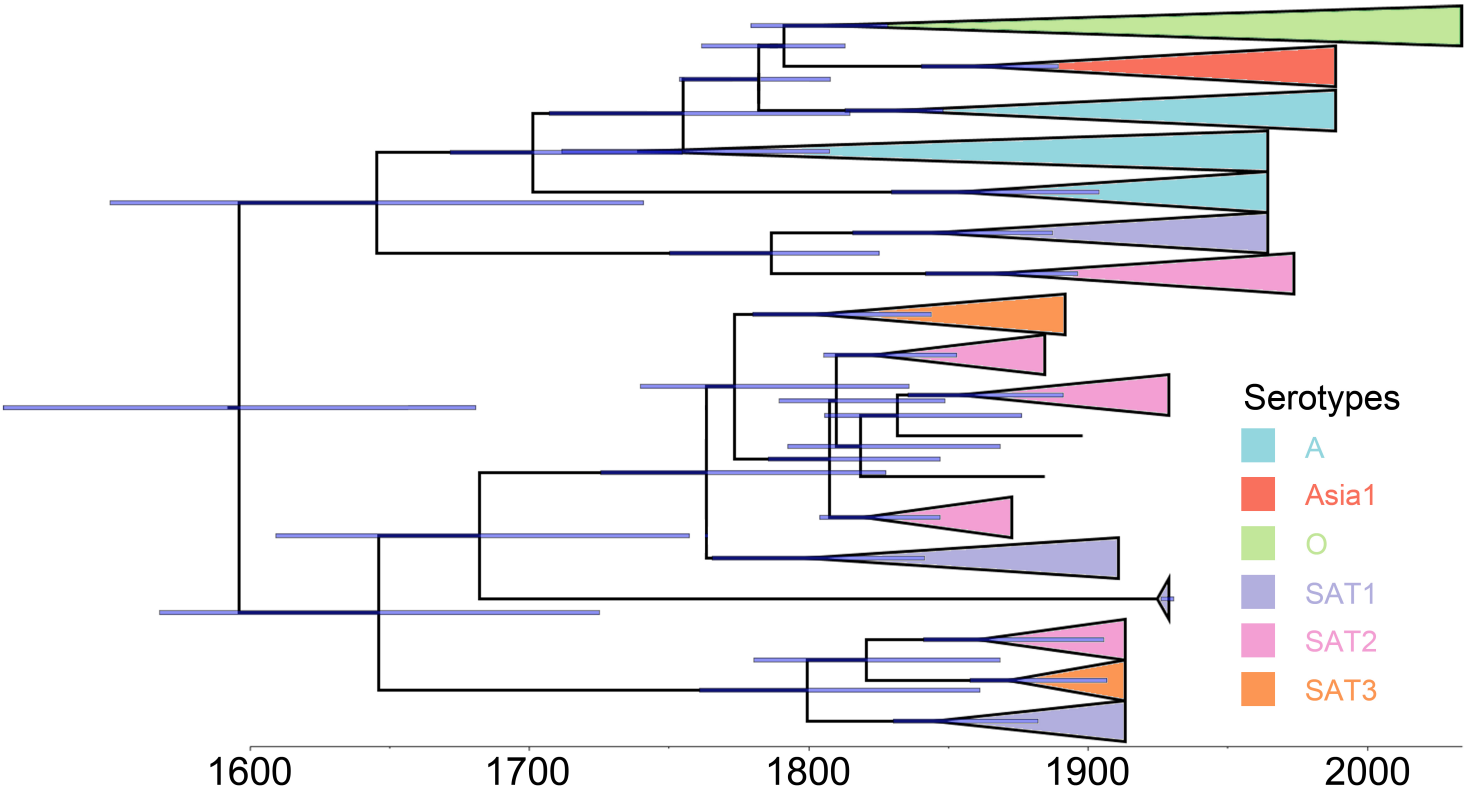

Figure 1

Condensed phylogenetic tree showing the overall evolutionary history of FMDV representing the relationships between all serotypes. The tree is based on a maximum clade credibility phylogeny inferred from 249 whole genome sequences. Branch bars represent posterior probabilities of branching events (P > 0.95).

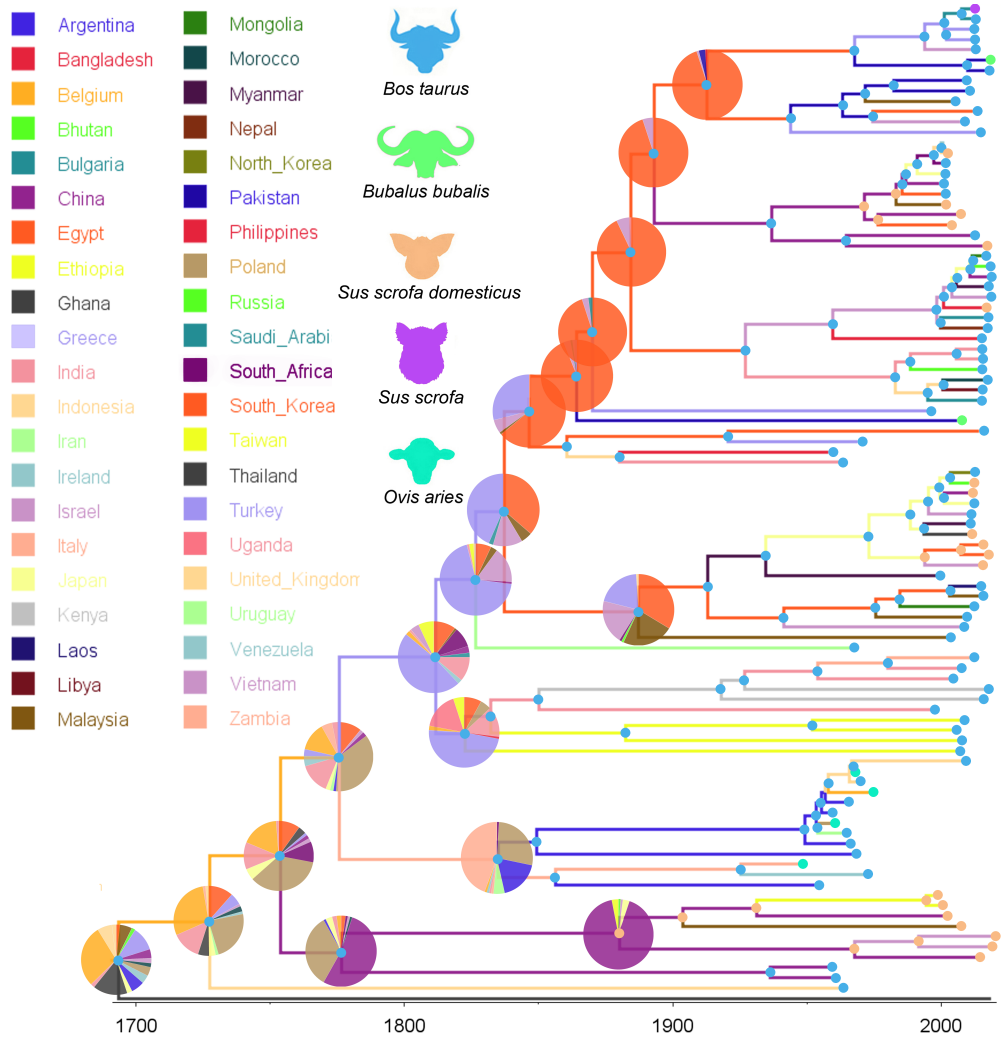

Figure 2

Dispersal history of FMDV lineages of Serotype O, as inferred by discrete phylogeographic analysis. Maximum clade credibility phylogeny colored according to the countries of origin. Branch bars represent posterior probabilities of branching events (P > 0.95). Colored dots at the end of the branches represent the host species (Bos taurus= cattle, Sus scrofa domesticus= swine, Ovis aries= sheep, Bubalus bubalis= water buffalo, and Sus scrofa= boar). The probabilities of ancestral states (inferred from the Bayesian discrete trait analysis) are shown in pie charts at each node, while circles on each branch and tips represent the most likely hosts.

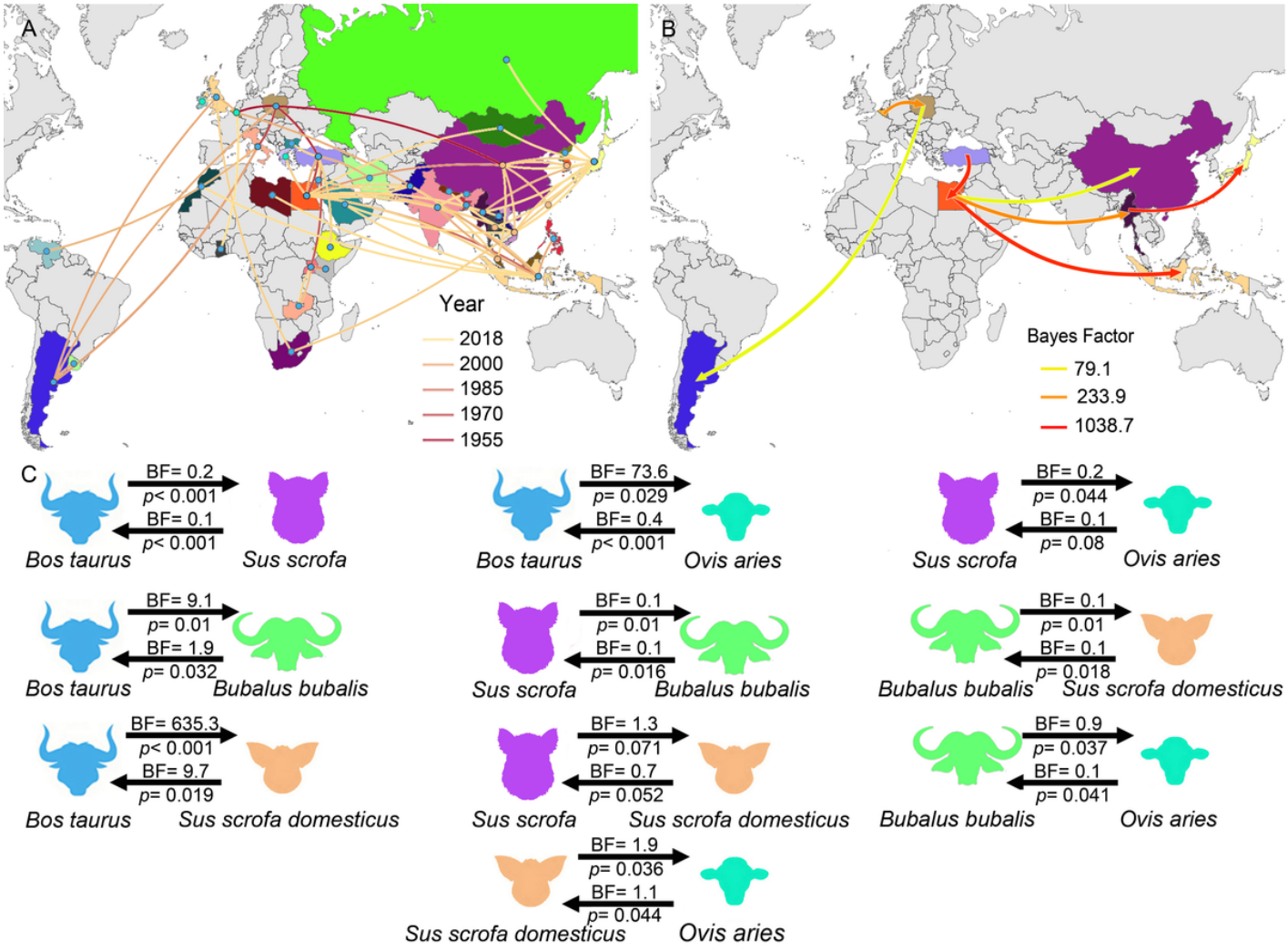

Figure 3

(A) Reconstructed spatiotemporal diffusion of FMDV serotype O spread, the color of the branches represents the age of the internal nodes, where darker red colors represent older spread events. (B) Representation of the most significant location transitions events for FMDV serotype O spread based on only the rates supported by a BF greater than 3 are indicated, where the color of the branches represent the relative strength by which the rates are supported. (C) Transmission rates between hosts (Bos taurus= cattle, Sus scrofa domesticus= swine, Ovis aries= sheep, Bubalus bubalis= water buffalo, and Sus scrofa= boar). based on BSSVS-BF values are represented on the top of the black arrows, while the root state posterior probability for the host-species transition are given on its bottom.

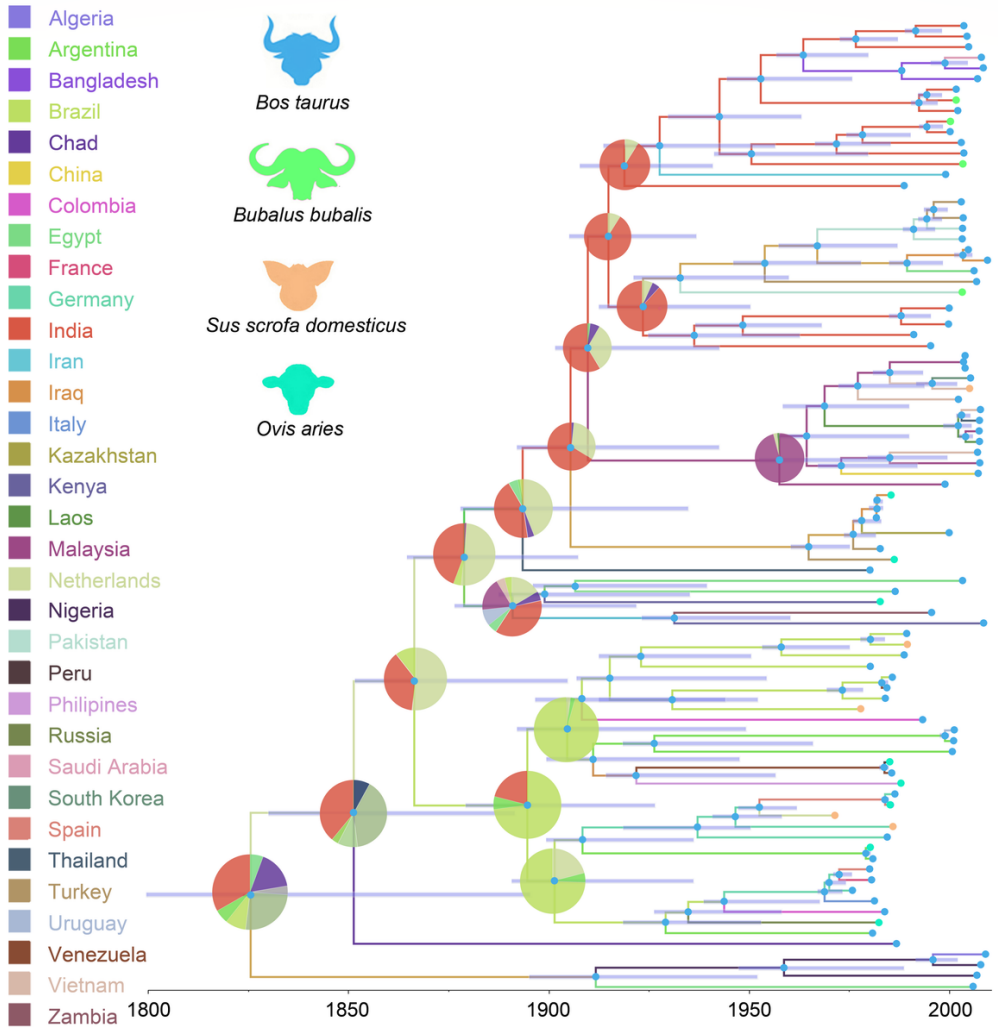

Figure 4

Dispersal history of FMDV lineages of Serotype A, as inferred by discrete phylogeographic analysis. Maximum clade credibility phylogeny colored according to the countries of origin. Branch bars represent posterior probabilities of branching events (P > 0.95). Colored dots at the end of the branches represent the host species (Bos taurus= cattle, Sus scrofa domesticus= swine, Ovis aries= sheep, and Bubalus bubalis= water buffalo. The probabilities of ancestral states (inferred from the Bayesian discrete trait analysis) are shown in pie charts at each node, while circles on each branch and tips represent the most likely hosts.

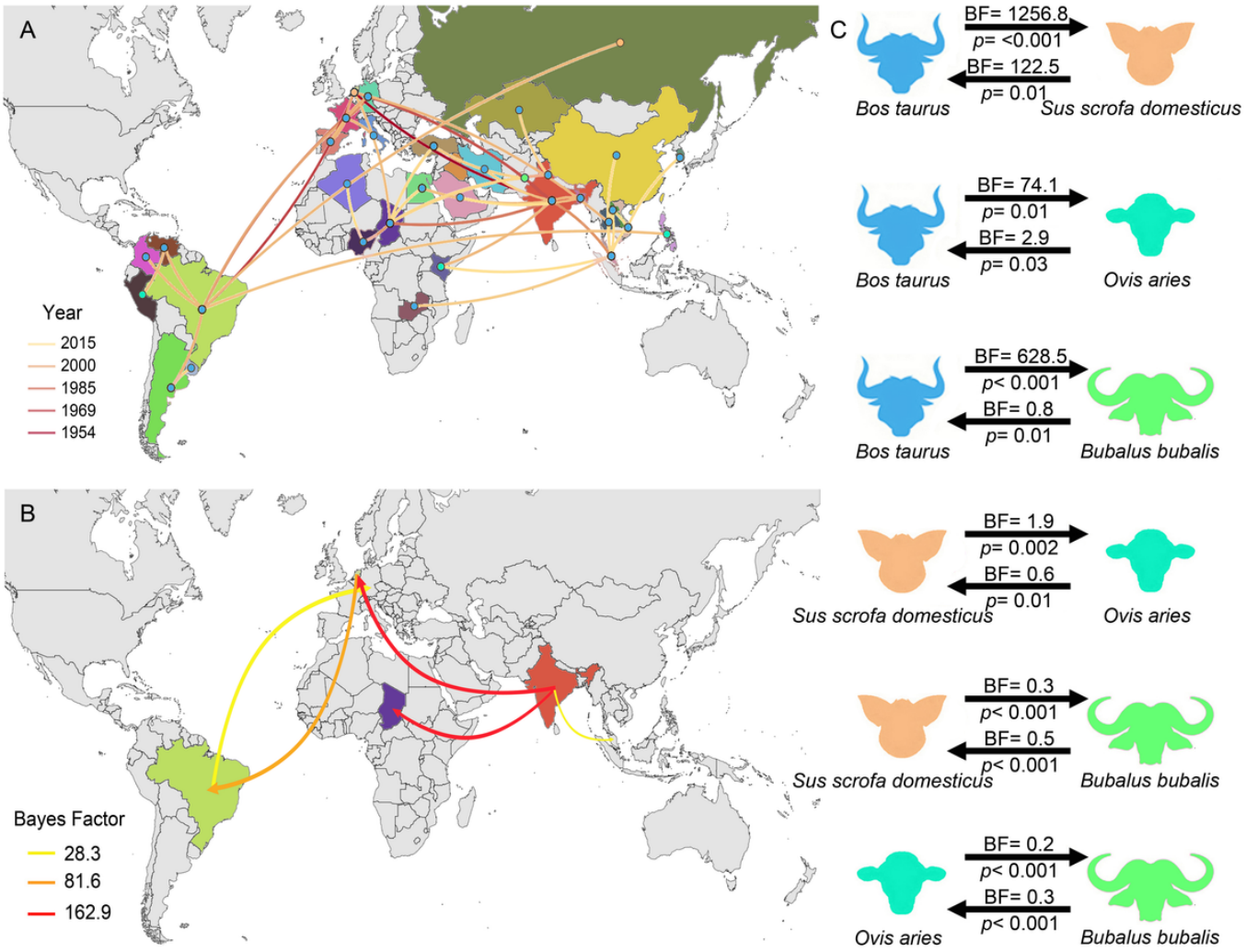

Figure 5

(A) Reconstructed spatiotemporal diffusion of FMDV serotype A spread, the color of the branches represents the age of the internal nodes, where darker red colors represent older spread events. (B) Representation of the most significant location transitions events for FMDV serotype A spread based on only the rates supported by a BF greater than 3 are indicated, where the color of the branches represent the relative strength by which the rates are supported. (C) Transmission rates between hosts (Bos taurus= cattle, Sus scrofa domesticus= swine, Ovis aries= sheep, and Bubalus bubalis= water buffalo) based on BSSVS-BF values are represented on the top of the black arrows, while the root state posterior probability for the host-species transition are given on its bottom.

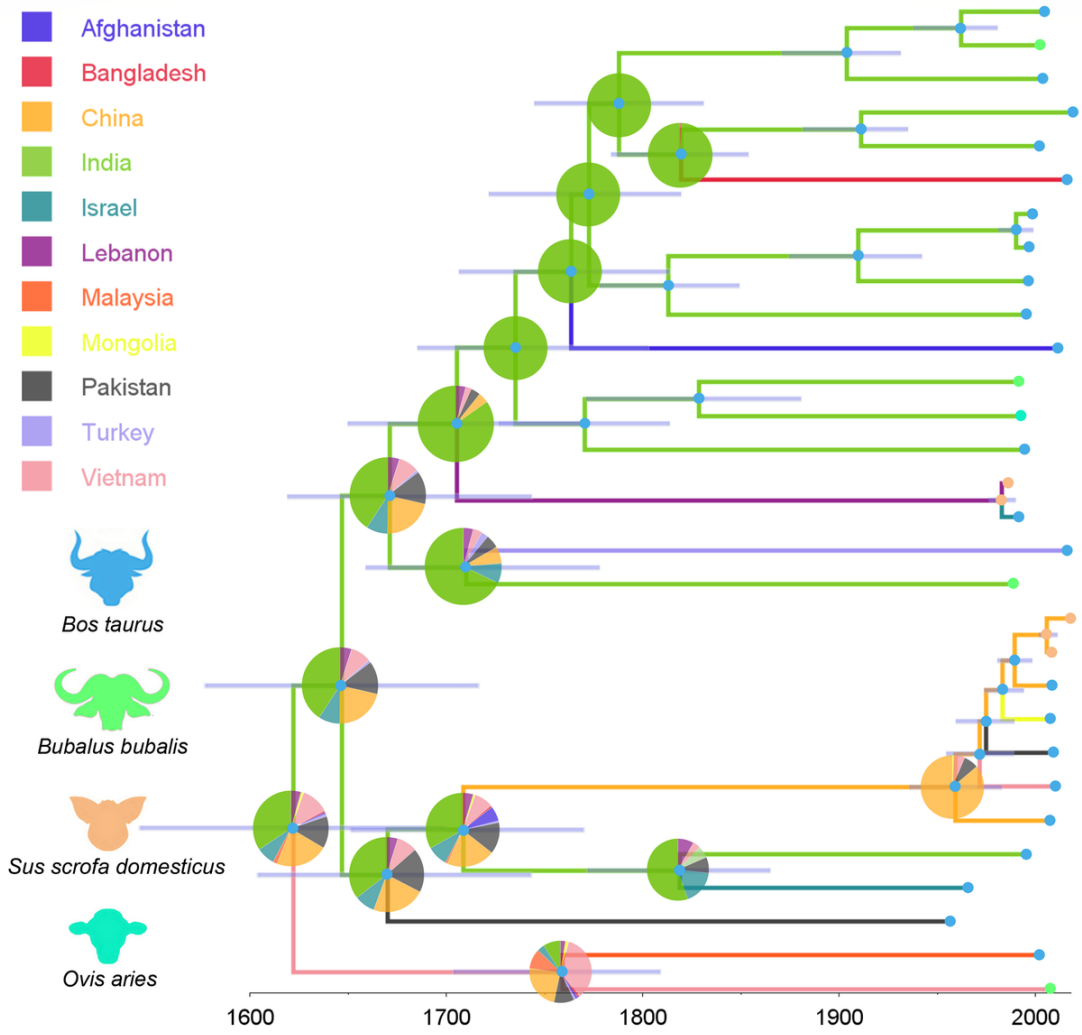

Figure 6

Dispersal history of FMDV lineages of Serotype Asia1, as inferred by discrete phylogeographic analysis. Maximum clade credibility phylogeny colored according to the countries of origin. Branch bars represent posterior probabilities of branching events (P > 0.95). Colored dots at the end of the branches represent the host species (Bos taurus= cattle, Sus scrofa domesticus= swine, Ovis aries= sheep, and Bubalus bubalis= water buffalo. The probabilities of ancestral states (inferred from the Bayesian discrete trait analysis) are shown in pie charts at each node, while circles on each branch and tips represent the most likely hosts.

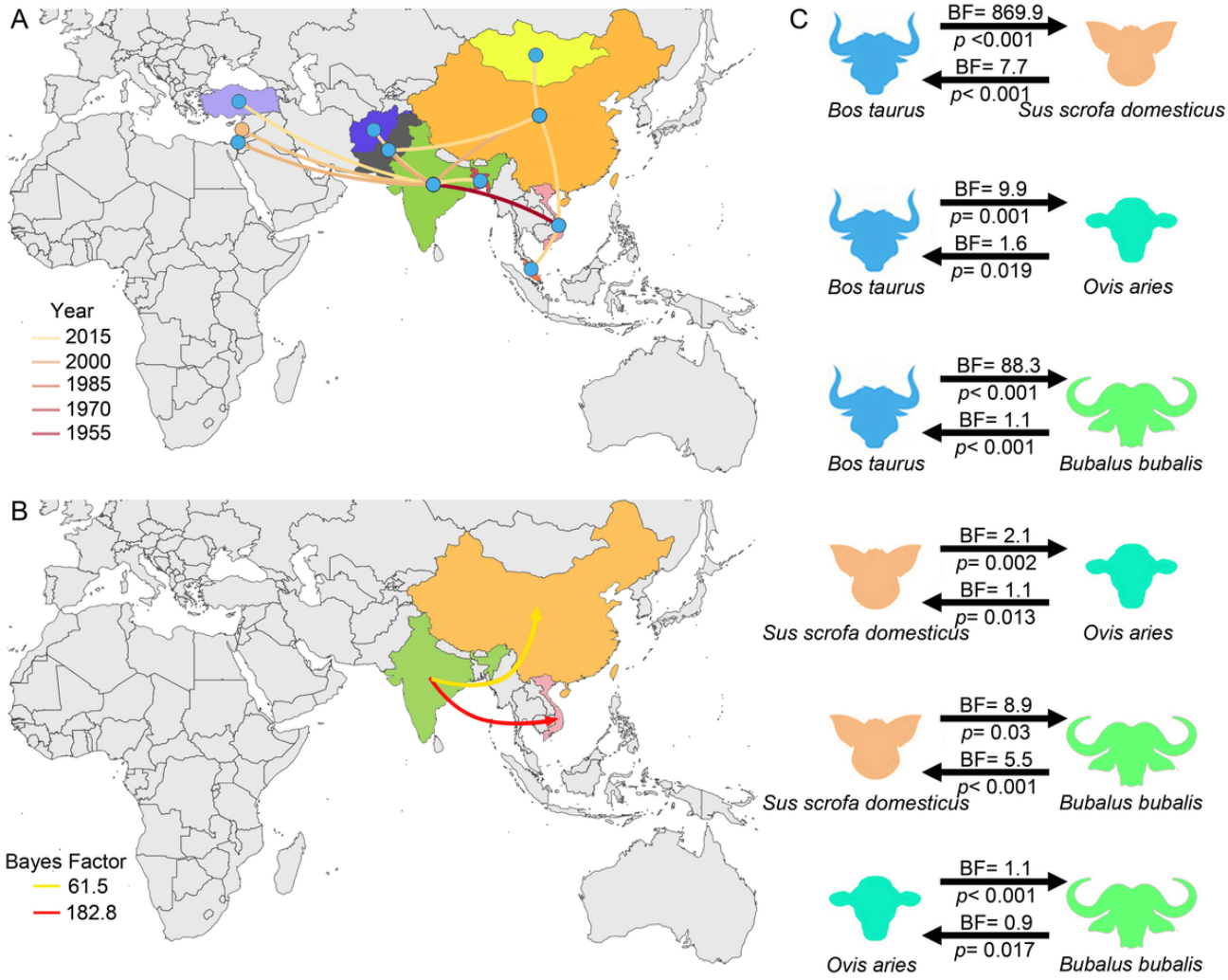

Figure 7

(A) Reconstructed spatiotemporal diffusion of FMDV serotype Asia1 spread, the color of the branches represents the age of the internal nodes, where darker red colors represent older spread events. (B) Representation of the most significant location transitions events for FMDV serotype Asia1 spread based on only the rates supported by a BF greater than 3 are indicated, where the color of the branches represent the relative strength by which the rates are supported. (C) Transmission rates between hosts (Bos taurus= cattle, Sus scrofa domesticus= swine, Ovis aries= sheep, and Bubalus bubalis= water buffalo) based on BSSVS-BF values are represented on the top of the black arrows, while the root state posterior probability for the host-species transition are given on its bottom.

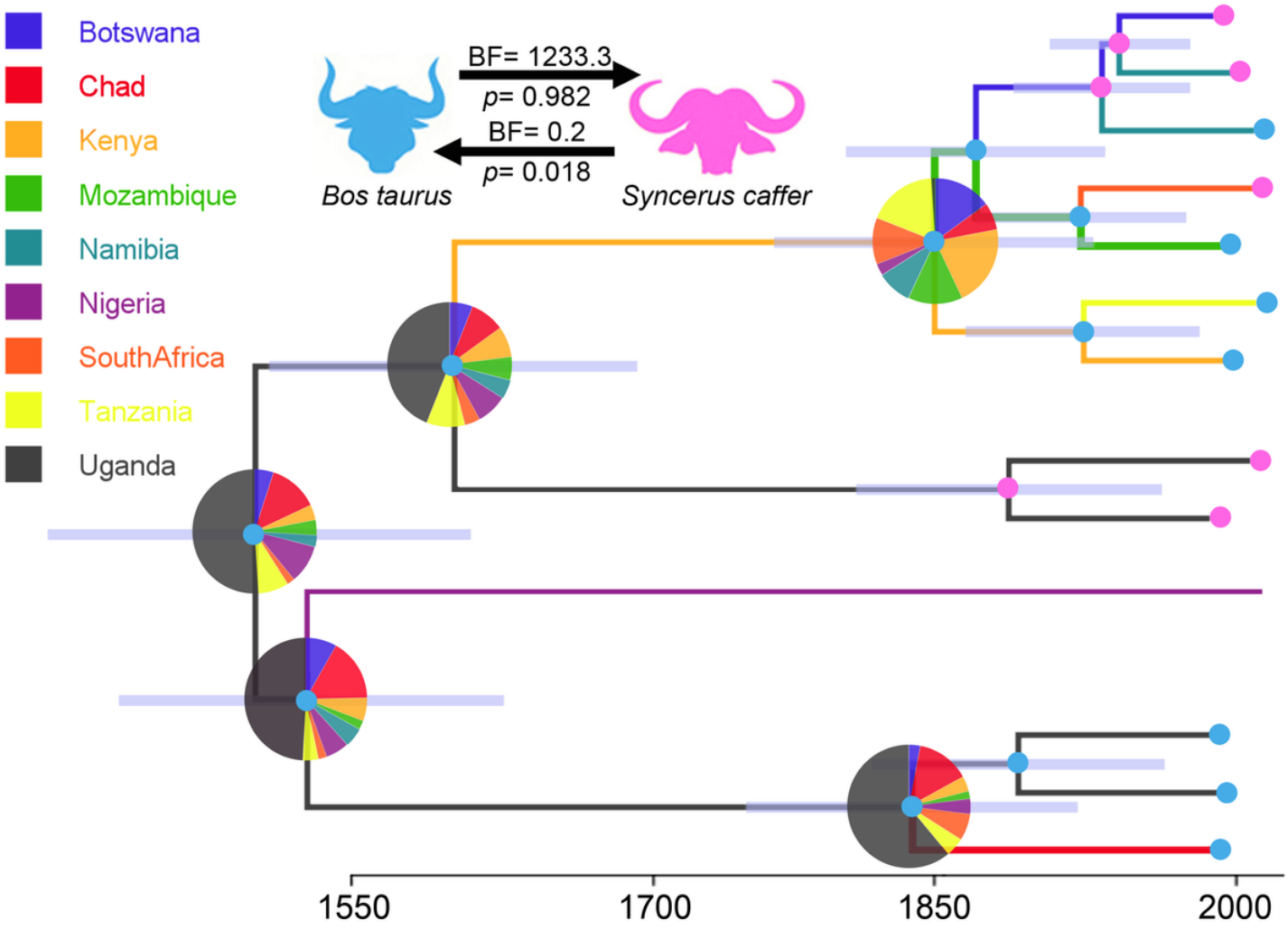

Figure 8

Dispersal history of FMDV lineages of Serotype SAT1, as inferred by discrete phylogeographic analysis. Maximum clade credibility phylogeny colored according to the countries of origin. Branch bars represent posterior probabilities of branching events (P > 0.95). Colored dots at the end of the branches represent the host species (Bos taurus= cattle, and Syncerus caffer= African buffalo. The probabilities of ancestral states (inferred from the Bayesian discrete trait analysis) are shown in pie charts at each node, while circles on each branch and tips represent the most likely hosts. Transmission rates between hosts (BSSVS-BF values) are represented on the top of the black arrows, while the root state posterior probability for the host-species transition are given on its bottom.

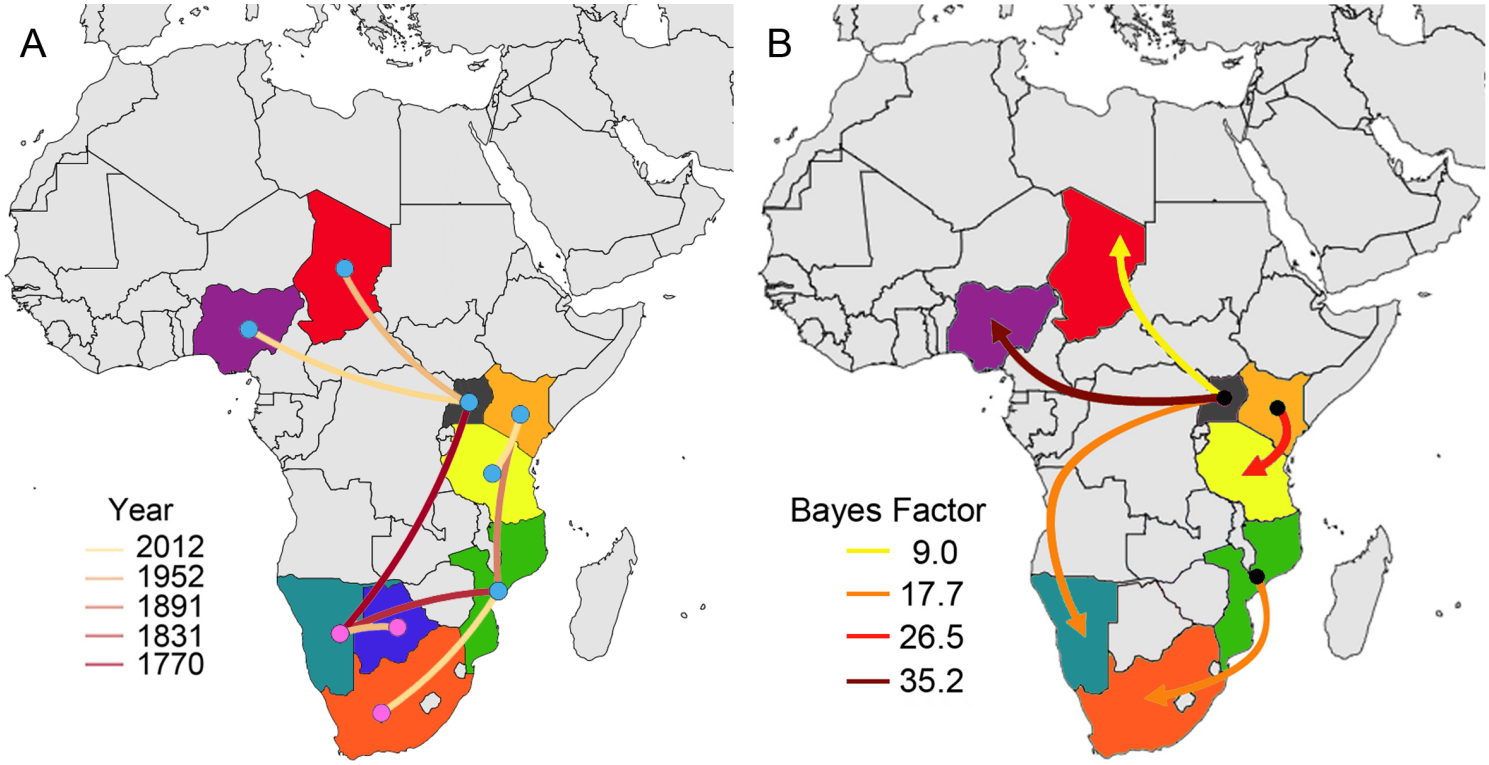

Figure 9

(A) Reconstructed spatiotemporal diffusion of FMDV serotype SAT1 spread, the color of the branches represents the age of the internal nodes, where darker red colors represent older spread events. (B) Representation of the most significant location transitions events for FMDV serotype SAT1 spread based on only the rates supported by a BF greater than 3 are indicated, where the color of the branches represent the relative strength by which the rates are supported.

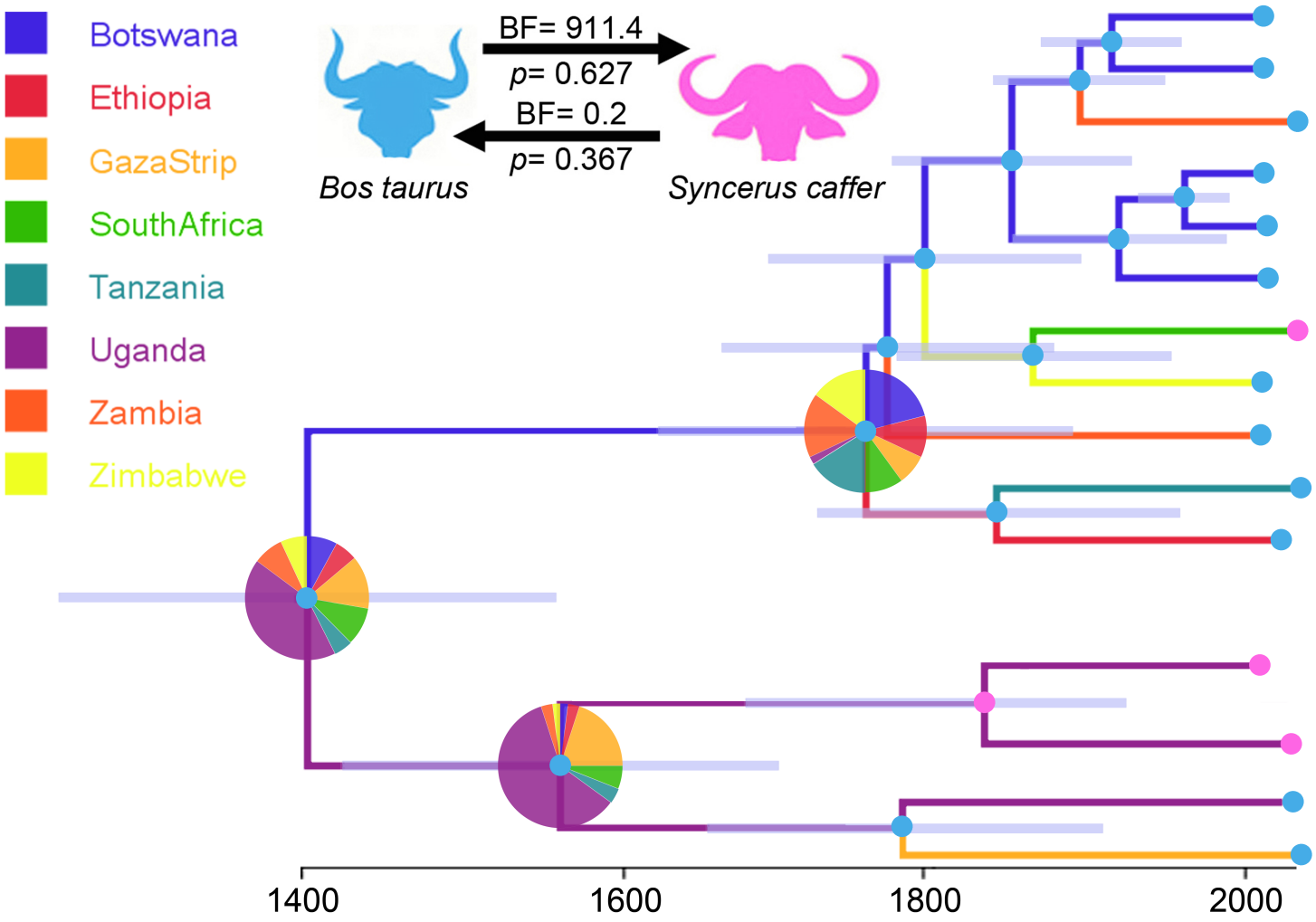

Figure 10

Dispersal history of FMDV lineages of Serotype SAT2, as inferred by discrete phylogeographic analysis. Maximum clade credibility phylogeny colored according to the countries of origin. Branch bars represent posterior probabilities of branching events (P > 0.95). Colored dots at the end of the branches represent the host species (Bos taurus= cattle, and Syncerus caffer= African buffalo. The probabilities of ancestral states (inferred from the Bayesian discrete trait analysis) are shown in pie charts at each node, while circles on each branch and tips represent the most likely hosts. Transmission rates between hosts (BSSVS-BF values) are represented on the top of the black arrows, while the root state posterior probability for the host-species transition are given on its bottom.

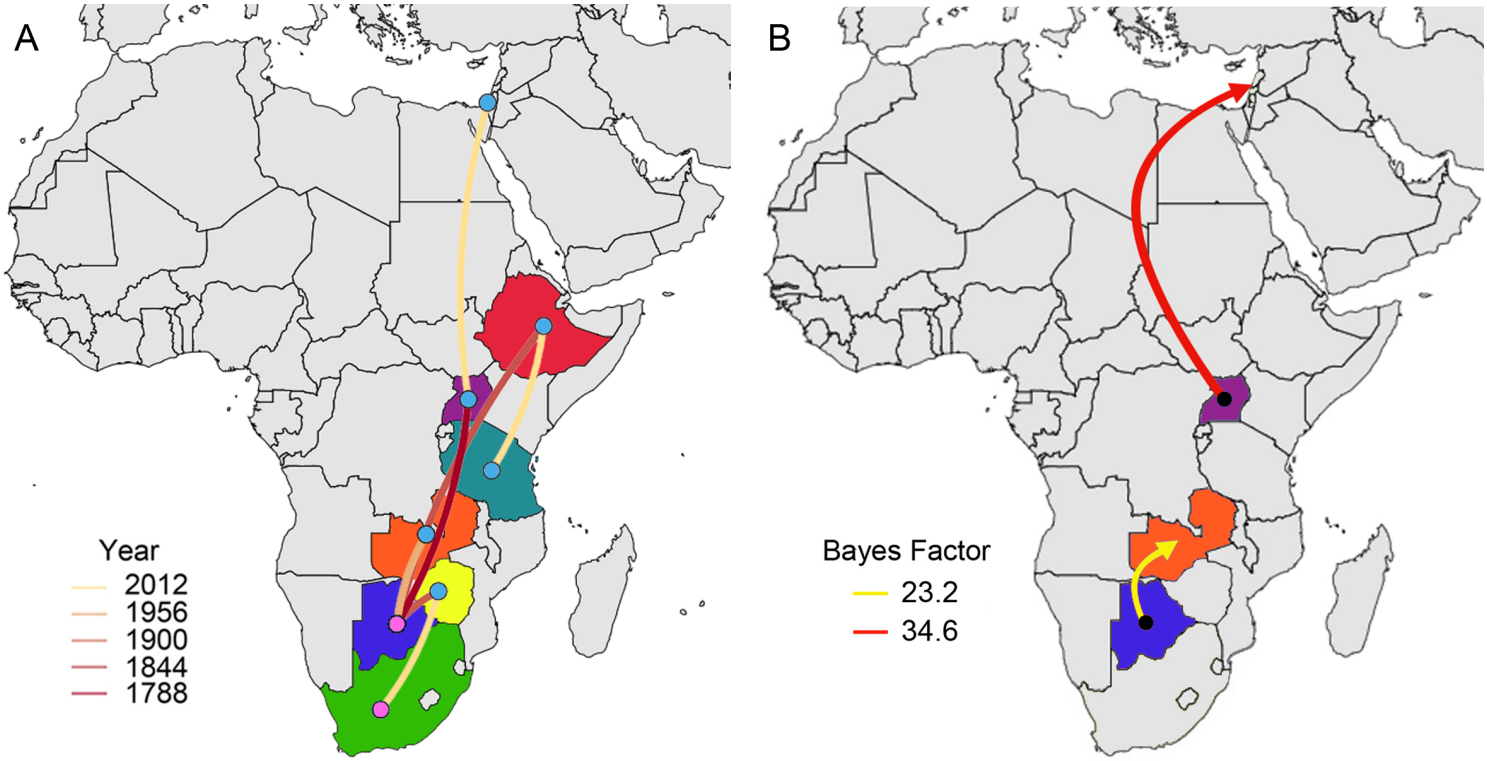

Figure 11

(A) Reconstructed spatiotemporal diffusion of FMDV serotype SAT2 spread, the color of the branches represents the age of the internal nodes, where darker red colors represent older spread events. (B) Representation of the most significant location transitions events for FMDV serotype SAT2 spread based on only the rates supported by a BF greater than 3 are indicated, where the color of the branches represent the relative strength by which the rates are supported.

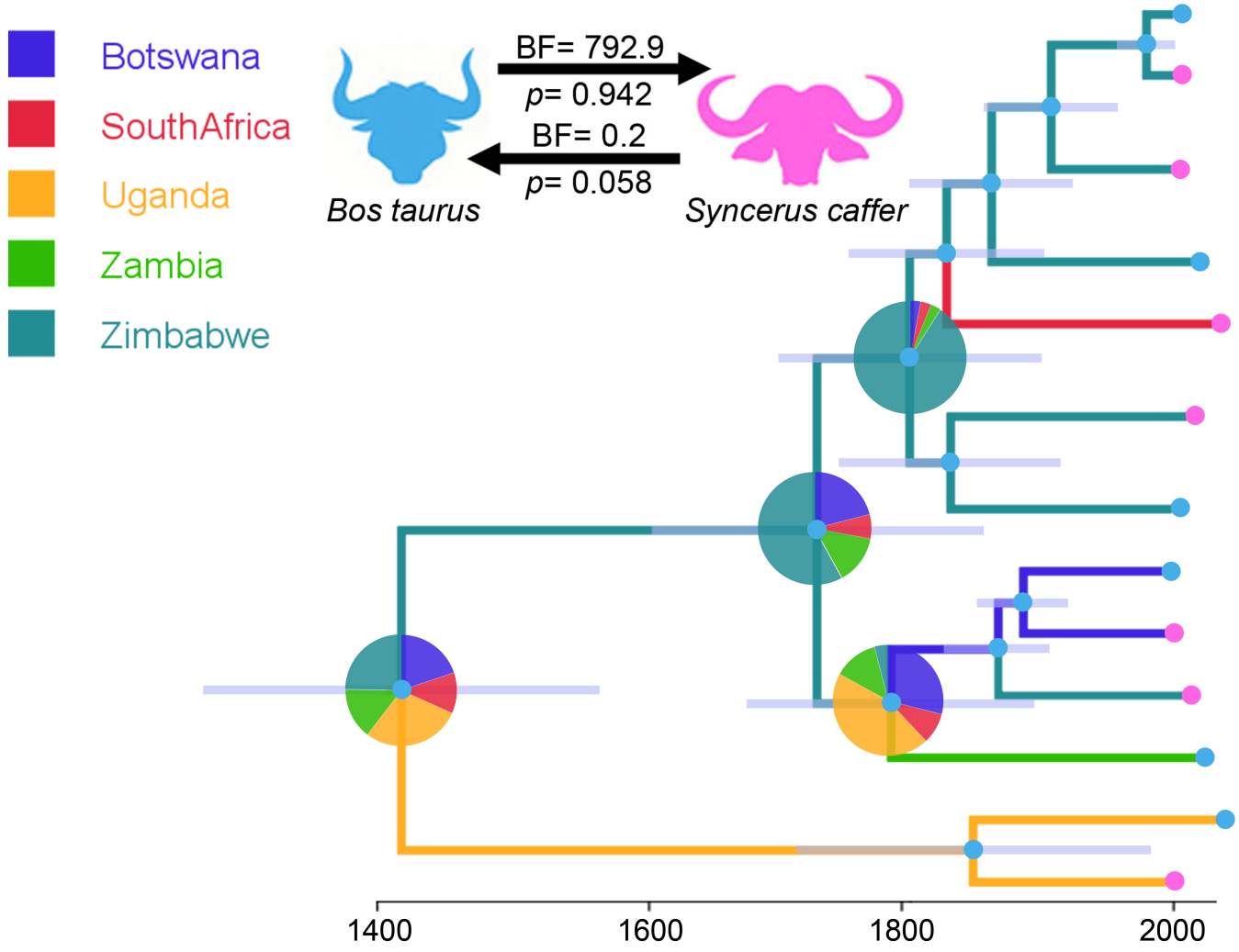

Figure 12

Dispersal history of FMDV lineages of Serotype SAT3, as inferred by discrete phylogeographic analysis. Maximum clade credibility phylogeny colored according to the countries of origin. Branch bars represent posterior probabilities of branching events (P > 0.95). Colored dots at the end of the branches represent the host species (Bos taurus= cattle, and Syncerus caffer= African buffalo. The probabilities of ancestral states (inferred from the Bayesian discrete trait analysis) are shown in pie charts at each node, while circles on each branch and tips represent the most likely hosts. Transmission rates between hosts (BSSVS-BF values) are represented on the top of the black arrows, while the root state posterior probability for the host-species transition are given on its bottom.

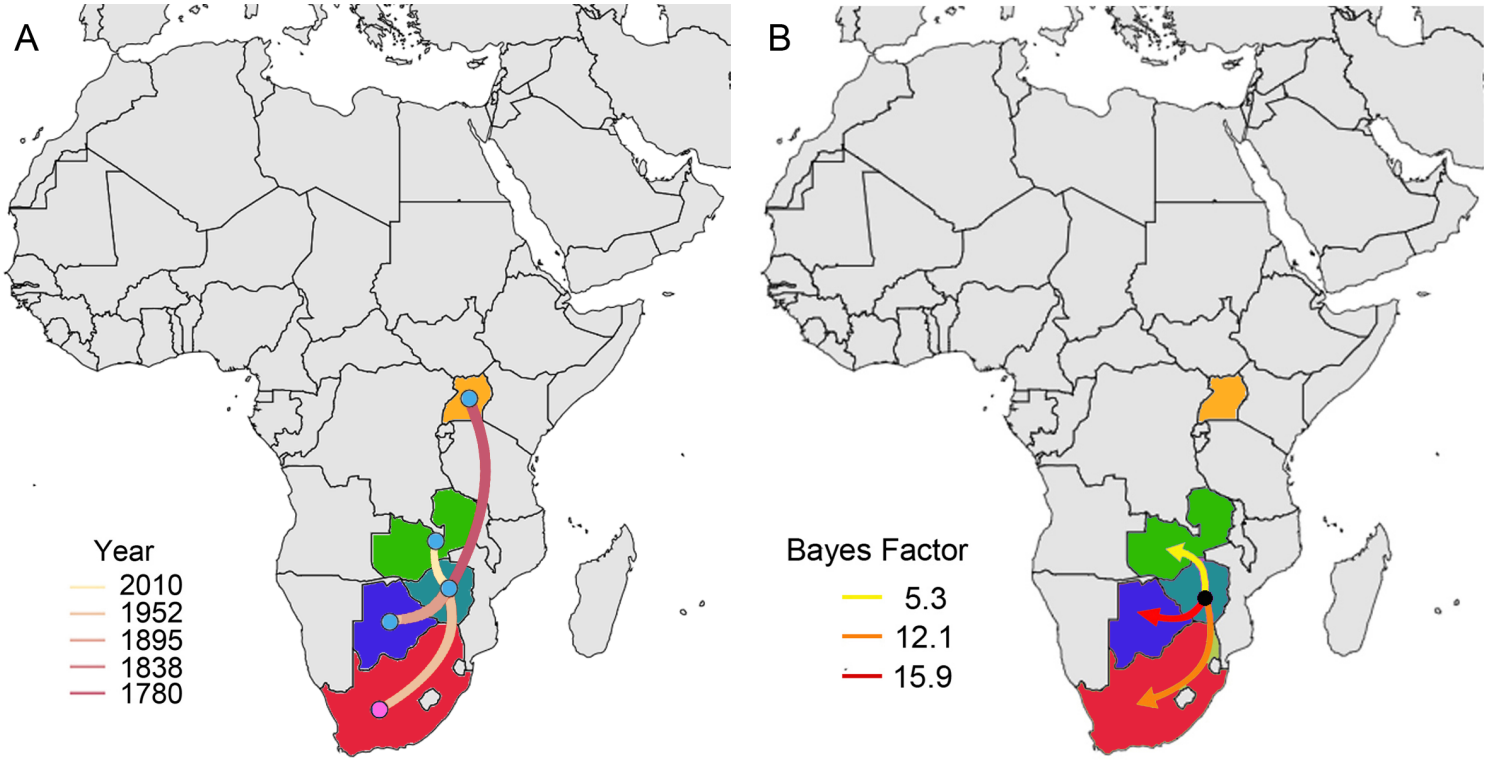

Figure 13

(A) Reconstructed spatiotemporal diffusion of FMDV serotype SAT3 spread, the color of the branches represents the age of the internal nodes, where darker red colors represent older spread events. (B) Representation of the most significant location transitions events for FMDV serotype SAT3 spread based on only the rates supported by a BF greater than 3 are indicated, where the color of the branches represent the relative strength by which the rates are supported.

Supplementary Files

This is a list of supplementary files associated with this preprint. Click to download.

- ARRIVEcheck.pdf
- S4FMDVSerotypeOspread.mp4
- S8FMDVSerotypeSAT3spread.mp4
- S5FMDVSerotypeAsia1spread.mp4
- FigureS2.jpg
- S7FMDVSerotypeSAT2spread.mp4
- S6FMDVSerotypeSAT1spread.mp4
- S3FMDVSerotypeAspread.mp4
- Supplementarymaterial12192019.docx
- Fig.S1Serotypespercountry.tif